MACHINING OF TITANIUM ALLOY (Ti-6Al-4V) - THEORY TO APPLICATION

A. Pramanik[1*], G. Littlefair[2]

[1]Department of Mechanical Engineering, Curtin University, Bentley, WA, Australia

[2]School of Engineering, Deakin University, Waurn Ponds, Australia

Abstract

This paper correlates laboratory based understanding in machining of titanium alloys with the industry based outputs and finds possible solutions to improve machining efficiency of titanium alloy Ti-6Al-4V. The machining outputs are explained based on different aspects of chip formation mechanism and practical issues faced by industries during titanium machining. This study also analyzed and linked the methods that effectively improve the machinability of titanium alloys. It is found that the deformation mechanism during machining of titanium alloys is complex and causes basic challenges, such as saw-tooth chips, high temperature, high stress on cutting tool, high tool wear and undercut parts. These challenges are correlated and affected by each other. Saw tooth-chips cause variation in cutting forces which results in high cyclic stress on cutting tools. On the other hand, low thermal conductivity of titanium alloy causes high temperature. These cause a favorable environment for high tool wear. Thus, improvements in machining titanium alloy depend mainly on overcoming the complexities associated with the inherent properties of this alloy. Vibration analysis kit, high pressure coolant, cryogenic cooling, thermally enhanced machining, hybrid machining and, use of high conductive cutting tool and tool holders improve the machinability of titanium alloy.

Key words: Titanium alloy, saw-tooth chip, high temperature, practical application

*Corresponding author
Phone: +61 8 9266 7981, Fax: +91 8 9266 2681, Email: alokesh.pramanik@curtin.edu.au

INTRODUCTION

Application of composite materials in aerospace industry has increased many folds in recent times. This could however not reduce the demand of some monolithic alloys, such as titanium alloys, in this field. Several superior properties, such as exceptional thermal resistance, high load bearing capacity and ability to resist corrosion, of these materials categorize them as superalloy. Aerospace components are generally made by removing huge amounts of swarf (chips) from large blocks of material. Near net shaping methods are very difficult for most of the aerospace components due to complex physical morphology, and high tolerance and superior surface finish requirements.

Workpiece materials vary widely in their ability to plastically deform, to fracture and to sustain stresses, strain, strain rate and temperature during machining (Bayoumi and Xie, 1995). Titanium alloys are generally accepted as "difficult-to-machine" materials. Low thermal conductivity and the volume specific heat of these materials result in high cutting temperature during machining. In addition, the ability of these materials to maintain strength at high temperature and severe work hardening lead to higher machining forces (Pramanik, 2013). Furthermore, the ability to change phase of titanium alloys makes the deformation process more complex. The hexagonal closed-pack (HCP) α and body centred cubic (BCC) β phases are crystal structures of Ti (Lutjering and Williams, 2003; Donachie, 1988). Pure Ti consists of 100% α phase at room temperature and transformation from α to β phase takes place at the β transus temperature 882°C. Vanadium (V) is added to pure Ti to reduce the β transus temperature for stabilizing the β phase and aluminium (Al) is added to increase the β transus temperature. Ti–6Al–4V consists of 6 wt% of Al and 4 wt% V. The β transus temperature of this composition is 995°C, beyond this temperature it is 100% β phase (Lutjering and Williams, 2003; Donachie, 1988).

The Ti alloy, especially Ti-6Al-4V alloy is the most attractive and commonly used metallic alloy in the aerospace industries (Kahles et al., 1985; Smith, 1981) and it is the main focus in this study. The machining for Ti-6Al-4V alloy is not very similar to machining of any conventional materials. The additional complexities in the machining of aerospace materials arise due to its response to the moving tool. For example, titanium alloys have a high yield stress to tensile strength ratio (>0.9), and the flow stress increases dramatically with strain rate, when strain rate is greater than 10^3 s^{-1} (Chichili et al., 1998; Ramesh, 2002; Follansbee

and Gray, 1989) which is easily achieved in any machining process. Twin-dislocation interactions significantly influence strain hardening during deformation of titanium alloy though the dislocation motion accounted for the majority of plastic deformation (Chichili et al., 1998). Thus, high temperature strength, very low thermal conductivity, relatively low modulus of elasticity, high strain hardening, poor dislocation motion through the microstructure and high chemical reactivity play important roles in machining mechanism of these alloys (Ginting and Nouari, 2006). For similar reasons the progress in the machining of titanium alloy has not kept pace with advances in the machining of conventional materials (Ezugwu and Wang, 1997).

Based on the inherent material hardness, many tools are capable of machining titanium alloys (Ti-6Al-4V). However, many of the harder tools, available in the market are not for this alloy due to chemical affinity which causes chemical wear in the cutting tools. Furthermore, chips weld easily on the tool to form build up edge (BUE). As a result, cutting tools wear rapidly through different wear mechanism during machining. Carbide tools are extensively used in aerospace industries. Very limited applications of modified ceramic tools are noticed in the research communities.

Machining of titanium alloys is a reasonably old topic (Shaw et al., 1954). There are many investigations considering different aspects of titanium alloy machining though there are reports of similar investigations by different researchers (Hartung et al., 1982, Jawaid et al., 1999, Turkovich et al., 1982). However, it is really a matter of arguments on how much of this laboratory based knowledge has been transferred to industries. So far, there have been huge investigations in machining of these materials but results and information are not well linked and the real picture of productivity improvement is not yet clearly visible. In addition, there is no detailed document to understand the machining behaviour and to get applicable practical data which are imperatively needed for the benefit of industry and research community. This paper investigates the machining mechanisms and correlates these with the machining outputs. It also suggests remedies to reduce machining cost and time based on the available understanding in literature from the industrial perspective. Finally, this investigation establishes correlation between the theory of titanium machining and its practical application.

DEFORMATION MECHANISM DURING MACHINING

Experimental understanding

The chip morphology is an important aspect that is commonly considered to evaluate the deformation mechanism of the machining process. Fig. 1(a) presents the typical morphology of the chip produced by machining of Ti-6Al-4V. Line A–B is the cross-section of the original undeformed surface and its length is characterised by L. The slipping angle (θ) is defined as the angle between the shear band and the tangent of the machined surface at the end of the shear band. Severe plastic deformation that occurred in a very narrow region is marked by C (Sun et al., 2009). All the chips that are obtained show a segmented morphology (Ginting and Nouari, 2006,). Cotterell and Byrne (2008) also obtained saw-tooth for cutting speeds from 4 to120 m/min and feeds of 0.05, 0.075 and 0.1 mm. As reported by several authors, such as, Ezugwu et al., (1997, 2003), segmentation is a characteristic shape of the chip when machining titanium alloys. The chips in Fig 1(a) were obtained at speed 1200 m/min and undeformed chip thickness 70 µm. Similarly, the chips in Figs 1(b) and 1(c) were obtained at speed 4800 m/min and, undeformed chip thickness 35 and 70 µm respectively. The Fig. 1 clearly shows that saw-tooth start to separate with the increase of speed (Fig. 1(a) and (c)) and undeformed chip thickness (Fig. 1(b) and (c)).

A segmented saw tooth chip which is produced during machining of titanium alloys is distinctly different to the ‘continuous’ or ‘uniform-shear’ chip (Barry et al., 2001). The mechanism of saw-tooth chip formation in machining titanium and its alloys is generally accepted to be based on the occurrence of thermo-plastic instability within the primary shear zone (Sheikh-Ahmad and Bailey, 1997; Bayoumi and Xie, 1995). The formation of the segments in saw-tooth chips consists of two main stages (Kamanduri and Turkovich, 1981). Those are (1) compression of the wedge shaped volume of material immediately ahead of the tool and (2) thermo-plastic instability by accommodating the further shear strain within the ‘failed’ shear zone. Thus segments with negligible deformation gradual build-up by the crushing or compressing of the work material ahead of the advancing shearing. With the advancement of crushing, the contact (between the segment being formed and the most advanced point of cutting edge) increases and relative motion (between the bottom surface of the chip segment being formed and the tool face) is negligible until the formation of segments. With the advancement of the cutting tool the new chip segments are gradually

formed and slowly push the previously formed chip segment along the rake face. This causes extreme shear between the segments in the primary zone. At this stage, the concentrated shear bands are observed between the segments in a longitudinal mid-section of (Fig. 1) a titanium chip (Komanduri, 1982).

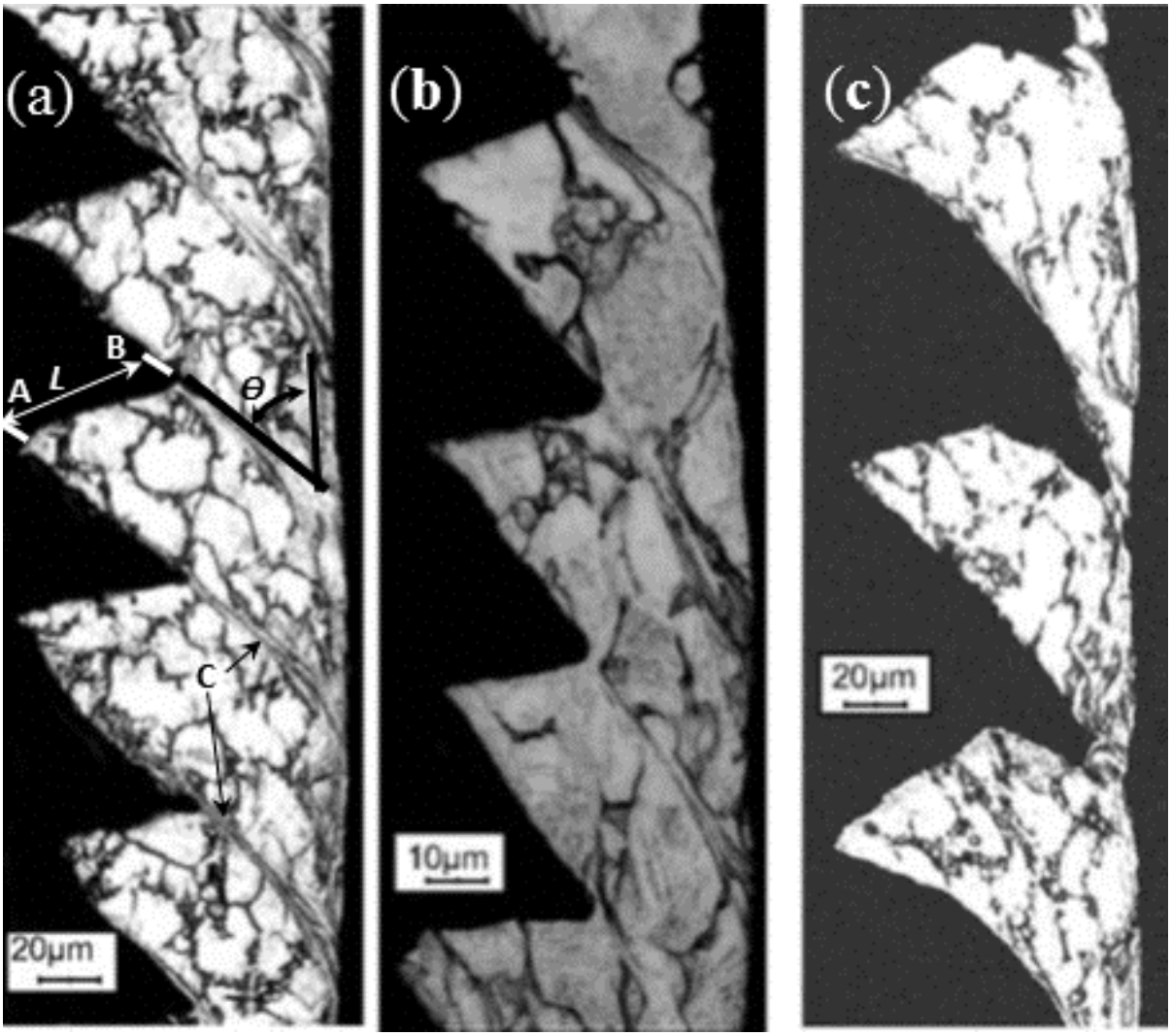

Fig. 1 Cross-sections of saw-tooth in machining of Ti-6Al-4V alloy (Gente et al., 2001).

The growth of cracks (Vyas and Shaw, 1999; Obikawa and Usui, 1996) and adiabatic shear band are caused by the localized shear deformation resulting from the predominance of strain hardening over thermal softening and minimum dislocation motion in the microstructure (Ginting and Nouari, 2006; Komanduri and Turkovich, 1981; Barry et al., 2001). During chip formation the crack starts in the primary shear zone towards the tool surface at low cutting speed (around 1.2 m/min) and the chip segments are separated from each other at the tool rake face but those are joined on the free surface. On the other hand, the cracks initiate in the

primary zone and propagate towards the free surface at higher cutting speeds (around 600 m/min). Thus chip segments are separated at the free surface but connected at the tool rake face (Shivpuri et al., 2002). The excessive shear localisation and strain hardening may be due to phase transformation of the titanium structure. Ti-6Al-4V alloy consists of lamellar α structure and intergranular β structure. In the chips, after machining loss of α structure takes place in the process of shear band formation due to transition from the hexagonal close packed (HCP) structure (α phase) to the body centred cubic (BCC) structure (β phase). This happens because of high pressure and temperature in shear zone. During this type of phase transformation, only grain change and no chemical composition change are noted. A new phase is also formed along the grain boundary through some relative movements of the grain boundaries (Komanduri and Turkovich, 1981; Bayoumi and Xie, 1995). This increases the number of available slip systems, and thus results in localised shear strain and increase shear hardening. The transition in the crystal structure presumably results primarily from the pressure and temperature increase which accompanies plastic deformation (Bayoumi and Xie, 1995; Barry et al., 2001). The β phase transition temperature of Ti-6Al-4V is approximately 1016 °C (Smith, 1981). Therefore, it follows that the temperature during machining this alloy reaches at least 1016 °C. The temperature can be very high and localised in some areas of the workpiece due to low thermal conductivity of Ti-6Al-4V alloy. This causes localised thermal softening which reduces the material strain-hardening capacity locally causing the shear instability in the narrow zones across the chip. The shear strain and plastic deformation in the shear banding area are much larger than in the area of the segments divided by shear bands (Bayoumi and Xie, 1995).

The onset of shear instability in chips depends on the cutting conditions and properties of the workpiece material (Komanduri and Hou, 2002; Bayoumi and Xie, 1995). It can be seen that the shear banding frequency increases as the feed rate increases or as cutting speed decreases. It appears that feed rate has a more significant effect on the shear banding frequency than does the cutting speed, although their effects are in opposite directions (Bayoumi and Xie, 1995). It is also found that shear localized chips are not always created at any cutting conditions. Continuous chips of a Ti-6A1-4V alloy are generated during machining at a relatively low cutting speed and feed rate. Usually, a critical cutting condition needs to be reached in order to have shear localized chips. There is critical cutting speed for the 'thermo-plastic' instability (adiabatic shear) to take place in machining Ti–6Al–4V (Barry et al., 2001;

Zhen-Bin and Komanduri, 1995). This critical cutting condition varies for different tool-workpiece material combinations (Komanduri and Hou, 2002) and depends on many other parameters, such as, cutting tool geometry, machine tool stability, etc. For Ti-6A1-4V alloy the saw tooth chips are generated when the product of feed (mm/rev) and speed (m/s) is around 0.004 or above (Bayoumi and Xie, 1995). It is evident that the transition from aperiodic to periodic saw-tooth chip formation is also effected by an increase in cutting speed and/or feed (equivalent to undeformed chip thickness in orthogonal cutting) (Barry et al., 2001). Cutting speed and feed significantly influence on chip morphology during machining of Ti alloy. Chips are mainly classified as either aperiodic saw-tooth or periodic saw-tooth; continuous chips were not produced within the range of cutting conditions employed; feed = 20–100 μm, speed = 0.25–3 m/s (Barry et al., 2001). (Bayoumi and Xie, 1995) calculated critical cutting conditions to form shear localized chips for different materials. For titanium critical cutting load, product of feed (mm/rev) and speed (m/s) is 0.004 which is lower than steel.

The roles of flow localization and adiabatic shear mechanisms are significant in the chip segmentation phenomena (Shivpuri 2002). Many researchers have investigated those roles. According to (Semiatin et al., 1983) the shear localization phenomena is related to the slope of the strain-strain rate curve. The shear localization occurs when this slope reaches 5 times the strain rate value. The applicability of this criterion was demonstrated on metalworking and metal cutting processes including titanium machining. (Hou and Komanduri, 1997) suggested the strain hardening and thermal softening regulate the stress in the localization region. The shear localization occurs when stress in the localized region is lower than that in the non-localized region. (Gente et al, 2001) studied chip morphological changes at very high cutting speeds (600 m/min, 1200 m/min and 4800 m/min) and established relationship between shear localization and chip fracture. It was suggested that the shear localization depends on the release of elastic energy and the strain in the localized zone or the cutting speed does not influence the fracture process. The underside of saw-tooth chips produced during machining Ti–6Al–4V alloy at high cutting speeds exhibit evidence of ductile fracture through void nucleation, growth and coalescence; the material between the voids necking down to a fine edge, resulting in a very distinctive directional structure.

Finite element simulation

The numerical tools have the capacity to simulate the chip formation of Ti64 alloy. Lin and (Lo, 1997) developed two dimensional cutting model and applied a line separation criterion for modelling the chip formation. According to their study, it seems that the variation of strain rate has a considerable effect on the results obtained. (Bäker et al., 2002) applied remeshing technique with an implicit scheme. (Umbrello et al., 2008) used the Johnson-Cook's (J-C) constitutive equation (Johnson and Cook, 1983) with three different set of material coefficients in a finite element analysis to simulate orthogonal machining of Ti-6Al- 4V alloy. Crockroft and Latham's damage criterion were applied in that simulation to obtain the segmented chip. The material coefficients which were taken from literature were found by the application of several methods (Lee and Lin, 1998; Meyer and Kleponis, 1998; Dumitrescu et al., 2002). It was seen the constants for J-C model obtained from split Hopkinson's bar tests (Lee and Lin, 1998) through high strain rate mechanical testing in a reasonable range of values (i.e. true strain, strain rate and temperature) provided reasonably good predictions in conventional as well as high speed machining. (Zhang et al., 2011) improved the friction contact model at tool/chip interface with a Lagrangian cutting model based on fracture energy damage growth. (Calamaz et al., 2008) introduced a new material model and took the strain-softening phenomenon into account in addition to strain rate hardening and the thermal-softening phenomenon. The new tool named TANH (Hyperbolic TANgent) added a new term to the Johnson–Cook's law in order to model the strain softening effect. The tool chip friction was introduced by a combined Coulomb–Tresca friction law. By introducing strain softening in the simulation, better prediction of chip morphology and strain field distribution was possible. The agreement between chip morphology is shown in Fig. 2. The agreement between numerical and experimental results depends on the selection of the Johnson–Cook's material parameters (Calamaz et al., 2008). (Karpat, 2011) studied the effect of various flow softening conditions on the outputs of finite element simulation during machining titanium alloy Ti-6Al-4V. Thus a new flow softening expression was integrated into the material constitutive model. This incorporated temperature-dependent flow softening behaviour during simulation. The flow softening was noted to initiate around 350–500°C and the outputs from simulation agree well with the experimental measurements (Karpat, 2011). Cutting model for Titanium alloys and based on crystal plasticity was reported by (Zhang et al., 2012). In this case, the grains were explicitly

taken into account, and their orientation angles and slip system strength anisotropy are considered as the main source of the microstructure heterogeneity. The continuum intra-granular damage model and the discrete cohesive zone inter-granular damage model were applied to simulate the material deformation process, and zero thickness cohesive elements were applied to simulate the bond at grain interfaces. The chip formation mechanism in the model developed by Zhang et al., (2012) described by shear slip between grains and by crystallographic slip within the grains very well. The different grain orientation angles lead to aperiodic chip segmentation for low cutting speed and feed rate. Segmented chip and micro-defects at its back become more pronounced at higher cutting speed. Micro-burrs and smoother cut are generated from intra-granular and inter-granular damages respectively (Zhang et al., 2012).

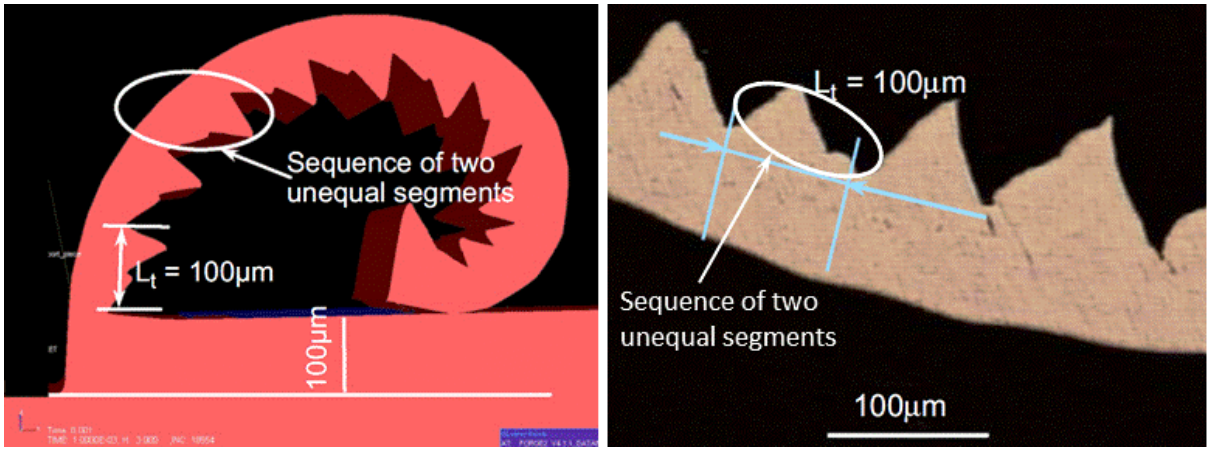

Fig. 2 Morphology of chips obtained from simulation (left) and experiments (right) (Calamaz et al., 2008)

OUTCOMES OF MACHINING

The investigations in machining of titanium alloy (Ti–6Al–4V) show that the outcomes and the causes of those outcomes are (1) the excessive shear localisation and strain hardening may be due to phase transformation of the titanium structure, (2) the 'thermo-plastic' instability (adiabatic shear) in machining Ti–6Al–4V takes place at critical cutting speed (3) the transition in the crystal structure presumably results primarily from the pressure and temperature increase which accompanies plastic deformation, (4) low thermal conductivity causes localised thermal softening which reduces the material strain-hardening capacity locally causing the shear instability in the narrow zones across the chip, (5) shear localization occurs when this slope reaches 5 times the strain rate value and (6) shear localization occurs

when stress in the localized region is lower than that in the non-localized region. All these can be described in details under following sections.

Saw-tooth chips

Generally, saw-tooth chips are formed during machining of titanium alloys. The saw-tooth chips have variable thickness. The chip length also changes with cutting speed. Short chips are produced at a lower range of cutting speeds, but the chips generated at higher cutting speed are much longer. The chip thickness in the continuous part is thicker than that in the segmented part. This suggests larger slipping between segments (Sun et al., 2009). The chip under higher magnification reveals different deformation processes for the segmented and continuous chips. In continuous chips the uniform shearing occurs continuously where the shearing plane makes smaller slipping angle (38°) with tool rake face. On the other hand, a narrow shear band with localised heavier deformation makes larger slipping angle (55°) with the rake face in the saw-tooth chips (Sun et al., 2009). It is already described in the preceding section that the critical cutting speed for the onset of shear instability and chip segmentation is very low during conventional machining of titanium alloy. At or above the critical cutting speed, segmented chip formation involves localized shearing which is associated with the cyclic variation of chip thickness. The cyclic variation in chip thickness generates cyclic variation in the machining forces (Sun at al., 2009) and acoustic emission. These dynamic cyclical and pulsating forces, and varying thickness, length and width of chips lead to machined surface, chatter and damaged cutting tool tip (Ezugwu and Wang, 1997; Komanduri and Hou, 2002; Abele and Fröhlich, 2008; Sun at al., 2009).

The formation of saw-tooth controls the behaviour of the dynamic cyclical and pulsating forces. The frequency of chip segmentation has similarity with the frequency of the cyclic forces and acoustic emission signal during machining (Vyas and Shaw, 1999; Barry and Byrne, 2001). In a range of cutting conditions, Sun et al., (2009) noted severe tool vibration at certain cutting conditions. The cyclic force frequencies are found to be approximately multiples of the intrinsic harmonic frequency (260 Hz) of the cutting when the machining process is stabilized. The cutting force and temperature increases with increase of cutting speed during machining titanium alloys. This makes it difficult to increase the machining speed of titanium alloys. The large force fluctuations (dynamic force) occurred due to formation of saw-tooth chips is superimposed on the static force (Sun et al., 2009). This

increases the deference between minimum and maximum forces during machining. In the periodic segmented chip region, the segmentation frequency can be calculated through dividing cutting speed by the length of undeformed surface (Barry and Byrne, 2001; Sun et al., 2009). The calculated segmentation frequency of chips agrees very well with the cyclic force frequency and indicates that the cyclic force fluctuation is caused by the segmented chip formation process (Vyas and Shaw, 1999; Barry and Byrne, 2001). Machining becomes stable when the frequency of these pulsating loads is in phase with the machine's natural frequency the variation of cutting forces. Otherwise, the self-excited chatter occurs which causes severe vibration and chatter.

High temperature

Harder materials usually produce higher machining temperature than the softer materials as the harder material has higher specific cutting energy. Generation of high temperature during machining any material is due to deformation and friction. The machining temperature is generally considered proportional to $u\sqrt{\frac{vf}{kpc}}$, where v is the cutting speed, f is the feed and u, k, p and c are the specific cutting energy, the thermal conductivity, the density and the specific heat of a workpiece, respectively (Shaw, 1984). It is thus related to cutting conditions and material properties. The machining temperature increases with the increase cutting parameters, such as speed and feed. On the other hand, the machining temperature increases with the decrease of the intrinsic properties of workpiece materials, such as the thermal conductivity, the density and the specific heat of a workpiece. Thus a smaller value of the product of these intrinsic properties of workpiece materials raises temperature even at a relatively lower machining speed and smaller feed (Kitagawa et al., 1997: Takeyama et al., 1983; Kikuchi, 2009). The magnitudes of density and thermal conductivity for titanium (thermal conductivity of titanium alloy is about 18.67 W/m °C at 1000 °C comparing to 381.77 W/m °C for steels) (Ginting and Nouari, 2006) are in favour to generate higher cutting temperature during machining processes. About 80% of the heat generated is conducted into the tool due to titanium's low thermal conductivity when machining Ti-6Al-4V. Fig. 3 shows that the thermal conductivity of titanium decreases with the increase of pressure and it has lowest thermal conductivity around temperature of 300°C. This indicates that the conductivity of titanium workpiece further decreases under cutting condition where high pressure is generally generated.

Thus, the properties of tool materials, especially the thermal conductivity, play a very important role when the product of *k*, *p* and *c* of workpiece material is very low. In case of high speed machining of aluminium almost all of the heat of machining is ejected with the chip during (Campbell, 2006). At a relatively low cutting speed (60 m/min), the temperature of the titanium alloy (Ti-6Al-4V) machining becomes higher than 1000 K and it can be as high as 1350 K at 200 m/min these are about 250 K higher than that of machining carbon steel. In case of medium carbon steel the temperature reaches only to 1123 K at the speed as high as 2400 m/min (Sutter et al., 2003). The heat generated during machining titanium stays mostly in the workpiece due to low thermal conductivity and ability to generate higher heat. While machining titanium alloy only the cutting edge of the tool takes parts in chip formation (Komanduri, 1982) and very high temperature is noted at the cutting edge (Ginting and Nouari, 2006). Accordingly, the heat stress becomes significantly higher when machining temperature is higher due to low heat dissipation by chips and the workpiece (Abele and Fröhlich, 2008). The distribution of temperature along the tool-chip interface at different cutting speeds is given in Fig. 4 (Abdel-Aal et al., 2009). The temperature generation the chip during formation is given in Fig. 5 (Calamaz et al., 2008). These show that the highest temperature occurs just at the cutting edge.

By the combination of low thermal conductivity and high thermal capacity, 30% more heat must be absorbed by the cutting edge compared to the machining of steel. The temperature at cutting edge is approximately double of that of steel when machining the Ti-6Al-4V (Abele and Fröhlich, 2008). Thus different types of cutting tool degradation processes, especially chemical reactions, are enhanced in this favourable environment (Abele and Fröhlich, 2008). These high cutting temperature and chemical reactions reduces tool life, surface quality and cutting accuracy due to thermal expansion of the tool and workpiece materials, and tool degradation (Kikuchi, 2009). In addition, localised nature of heat generation reduces the material strain-hardening capacity locally causing the shear instability in the narrow zones across the chip. The shear instability causes variation of uncut chip-thickness which leads to variation of localised machining temperature. Therefore, a noticeable cyclic thermal stresses are expected when the variation of feed is reasonably high. Among the machining parameters, the effect of speed is the most significant on machining temperature. The machining temperature increases with the increase of speed and feed (Ginting and Nouari, 2006). A lower cutting temperature is desired for better machinability of titanium as the

inherent high chemical reactivity of titanium at elevated temperature also worsens the problem (Kikuchi, 2009).

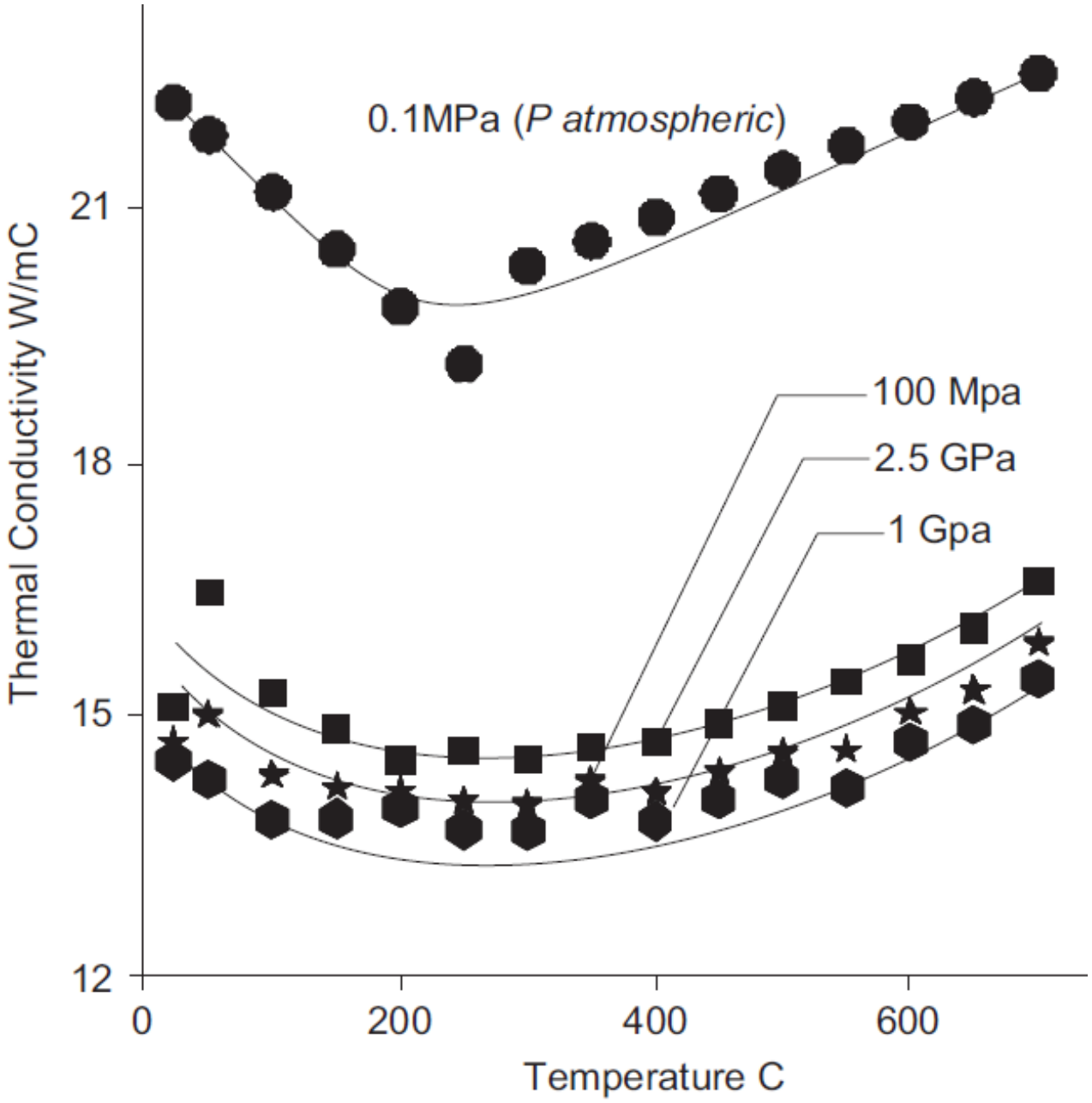

Fig. 3 Effect of pressure and temperature on the thermal conductivity of titanium (Abdel-Aal et al., 2009)

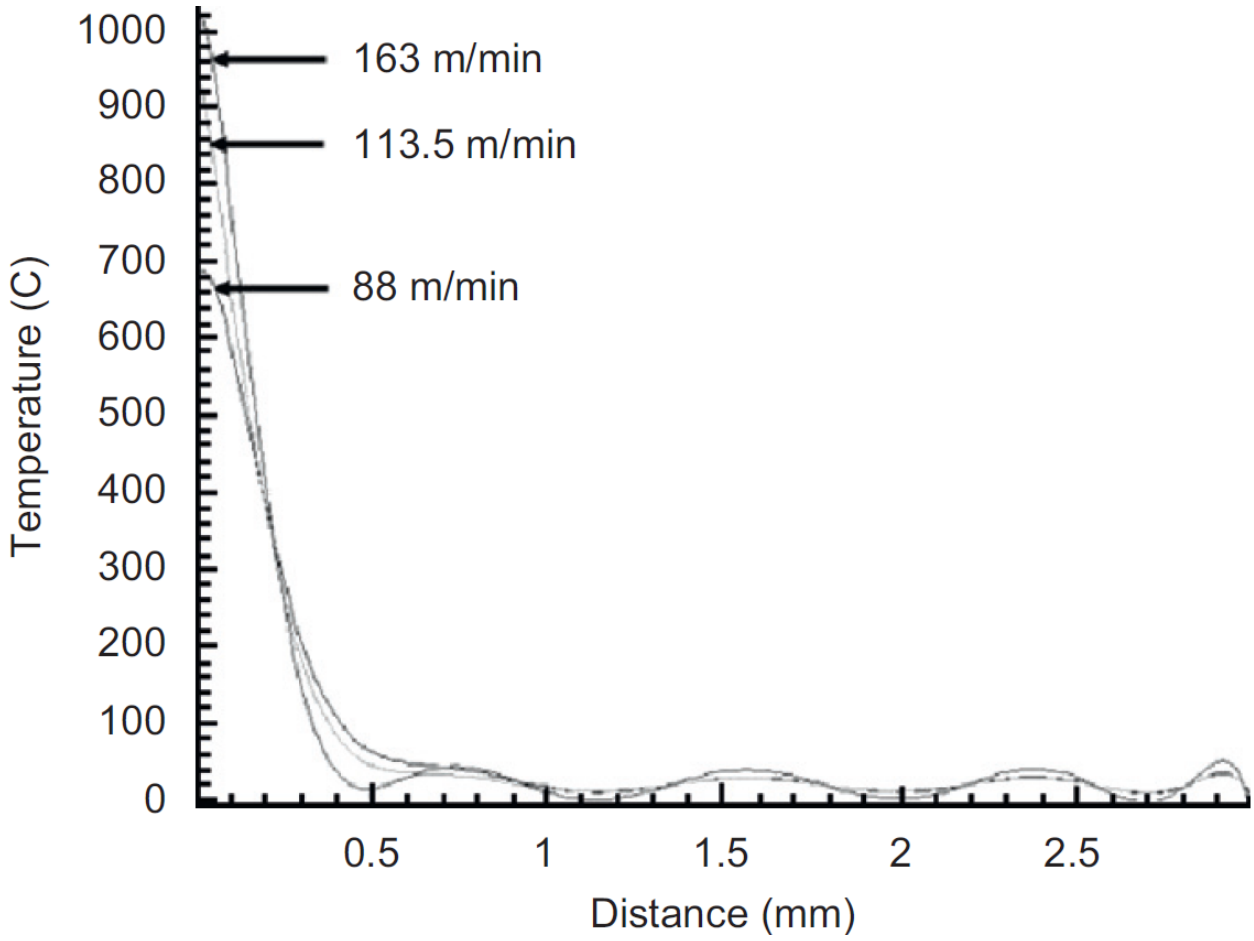

Fig. 4 Cutting temperatures at the tool–chip interface when end milling at tooth feed of 0.15m/tooth, as a function of distance from the tool cutting edge (Abdel-Aal et al., 2009).

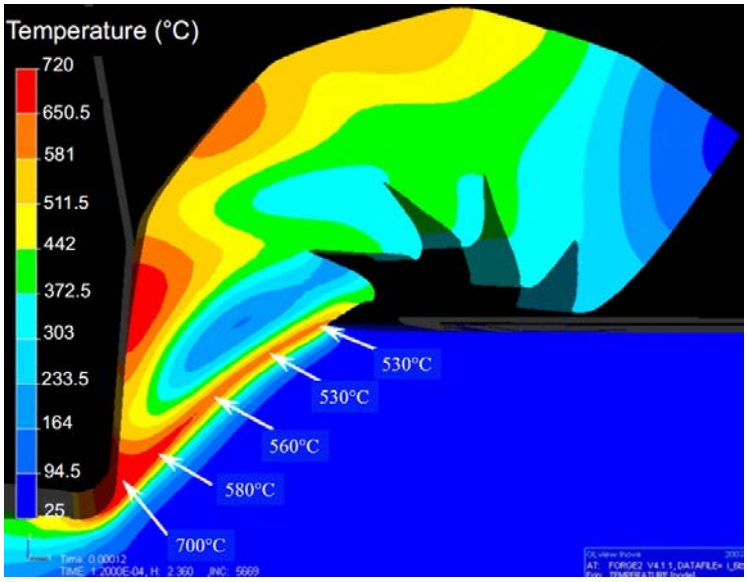

Fig. 5 Temperature evolution into chip for Cutting speed 180 m/min and feed 0.1mm (Calamaz et al., 2008)

High stress on cutting tools

High stress on the cutting edge is due to reduced contact surface and low plasticity of titanium alloys (Abele and Fröhlich, 2008). It is already explained that the segments in chip generation involve gradual upsetting of the wedge shaped volume of material immediately ahead of the tool due to formation of saw-tooth. Fig. 6 presents a picture of typical stress distribution on the cutting tool tip when saw tooth chips are formed (Duan, et al., 2013). It shows that the highest stress occurs at close proximity to the cutting edge. The maximum stress occurs within 0.1 mm from the cutting tool tip. The cutting tool geometry significantly influences the stress generated during machining (Wyen, et al., 2010). There is no stress after around 0.3 mm away from the tool tip when the rake angle -10° and this distance can be around 0.2 mm for 0° rake angle. This distances decreases with the increase of rake angle. Thus, the initial contact time and length on the tool face with the chip being formed is extremely small. Upsetting of the wedge shaped volume of material being formed causes high stress on the tool face owing to the small contact area. Thus, very high mechanical stresses occur in the immediate vicinity of the cutting edge when machining titanium (Campbell, 2006). Though the contact length increases as the chip formation process continues (Komanduri, 1982) the maximum force acts near the cutting edge (Ulutan, et al., 2013). The stress on cutting edge also increases with an increase in cutting speed due to the decrease of the associated contact length and shear angle (Ginting and Nouari, 2006; Jawaid et al., 1999). This mechanism is different from that of the continuous chip formation process (Komanduri, 1982). The stress on the rake and flank faces of a carbide tool during machining can be as high as 2600 and 1710 MPa respectively at speed 70 m/min and 0.1 mm feed (Ulutan, et al., 2013). The strength and hardness of titanium does not reduce significantly at elevated temperatures which contribute to higher stress at higher temperature on cutting tools (Campbell, 2006). Thus, cutting tools have to go through extreme stress conditions when machining titanium and wear out rapidly. The normal stress increases leading to a long intimate contact between the chip and rake surface as the rake angle decreases yielding higher apparent coefficient of friction.

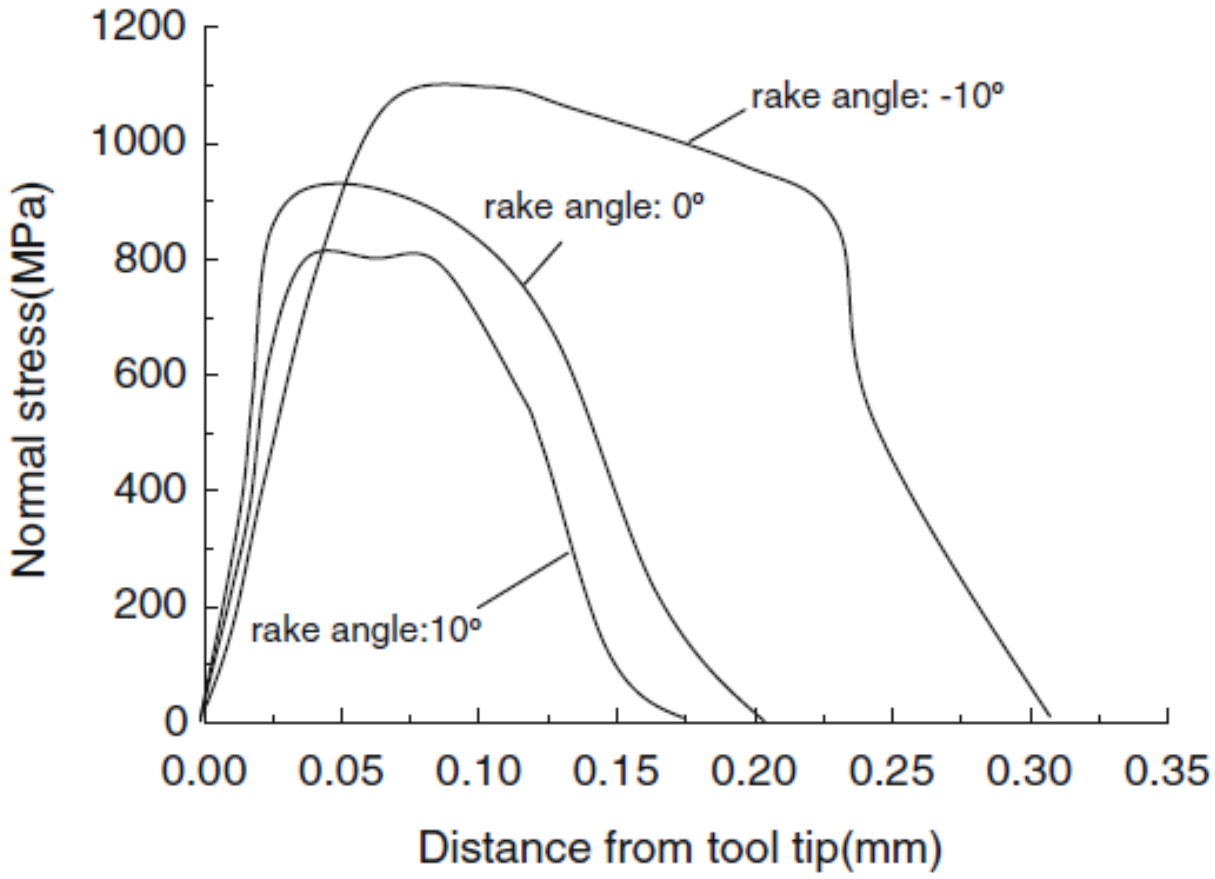

Fig. 6 Normal stress for saw-tooth chips at chip–tool surface for different rake angles (Duan, et al., 2013)

High tool wear

The above sections already described that cutting tool has to go through sever adverse environment during machining of titanium alloy. High and pulsating pressure, and high temperature and friction create an environment where degradation of cutting tools is accelerated. The following paragraphs give details of tool material and wear during machining of titanium alloy.

High speed steels (HSS) tool, such as M33, M40, and M42, and tungsten carbide grade C-2 (ISO K20) cutting tools are mainly used for machining titanium and its alloys in industries. Though carbides are susceptible to chipping during interrupted machining it can achieve about a 60% improvement in metal removal rates compared to HSS (Campbell, 2006). Ceramic cutting tools are not generally used in machining titanium due to low fracture toughness, poor thermal conductivity and higher chemical reactivity with titanium. Cutting

tool materials and coating technology contributed tremendous productivity improvements in machining for several materials (e.g., steels) but these achievements could not contribute significantly to improve machining of titanium and its alloys (Campbell, 2006). However, researchers in laboratory have tested all most all types of cutting tools, such as straight tungsten carbide tool (k10), cemented TiN tool, pure aluminium oxide type of ceramic tool, TiC coated tool, alloyed cemented carbide (W–Ti/Ta)C–Co, alloyed CVD-coated carbide (W–Ti/Ta/Nb)C–Co + (TiC+ Ti/CN + /TiN), CBN (American) tool, binderless CBN, sintered diamond tool and natural diamond tool (Takeyama et al., 1983; Haron et al., 2007; Takeyama et al., 1983; Jawaid et al., 1999; Jawaid et al., 2000; Jianxin et al., 2008; Rahman et al., 2006). The following discussion provides details on the performance of different kinds of cutting tool while machining titanium alloy (Ti-6Al-4V).

Excessive wear which is identified as chemical reaction and adhesion between the tool and work materials occurs in TiN added cermet and the TiC coated tools during machining. The ceramic and CBN tools also show large groove wear on the flank and rake face. Thus, these tool materials are not suitable for machining titanium alloys. However, only the carbide, sintered diamond and natural diamond tools show acceptable performance in machining titanium alloy. In addition, binderless CBN shows promising results in machining titanium alloys. The sintered diamond tool performs slightly better than its carbide contemporary at low speed but at higher speed both of these tools demonstrate almost similar performance. Tungsten carbide (k10) tool wear increases rapidly after 5 minute cutting at low speed (100 m/min) without coolant (Takeyama et al., 1983). However, the wear rate with the water-soluble type coolant is significantly low even after 30 minute cutting. At higher cutting speeds (198 m/min), the tool life becomes extremely short. On the other hand, natural diamond tooling showed minor wear even after 30 minute cutting at low (100 m/min dry) as well as at higher (198 m/min with coolant) cutting speeds. However, the tool wear was severe with further increase of cutting speed (300 m/min) even after cutting for only a few minutes. The other weakness is the low melting point of soldering material of natural diamond tool. If the machining is continued for long enough the soldering material melts and the cutting tip detaches from the holder (Takeyama et al., 1983). Polycrystalline cubic diamond (PCD) tooling shows very good performance during finish milling of low stiffness components of titanium alloy TiAl6V4. The tool life of PCD tooling can be achieved as high as 381 minutes with excellent surface finish and geometrical accuracy (Kuljanic et al., 1998). (Kuljanic et al.,

1998) down milled TiA16V4 titanium with 32 mm diameter PCD tool at cutting speeds 90, 130 m/min, feed per tooth 125 mm, axial depth of cut 0.3 mm and radial depth of cut 5 mm. For their specific machining condition, 10° inclination of the cutter axis to the surface perpendicular to the machined surface and application of cooling lubricant (7% oil and water) provided best machining out comes. Generally, diffusion and dissolution processes are blamed for damage of PCD tooling due to high local temperatures resulting from the poor thermal conductivity of workpiece materials (Nabhani, 2001). (Kuljanic et al., 1998a) argued that Ti has greater affinity to carbon. Thus, TiC film is formed on the diamond surface due to reaction between the work material and tool material during machining process. This film protects the tool from cratering under light cutting conditions.

Binderless CBN tools which do not have any binder present to hold the tool material grains together show an improved high temperature durability and thermal conductivity (Rahman et al., 2006). These tools are manufactured by direct sintering of high-purity hexagonal boron nitride (hBN) at high temperature and pressure. For the similar machining conditions (speed 400 m/min, feed 0.058 mm/tool and depth of cut 0.05 mm) the tool life of a BCBN tool is very similar to that of PCD tools during milling Ti-6Al-4V (Zareena, 2002). BCBN tools exhibit lower flank wear and sharper cutting edge compare to that of sintered carbide, PCBN and PCD (with Co based binder) tools during turning of Ti6Al2Nb1Ta at speed 4.2 m/s, feed 0.15 mm/rev and depth of cut 0.5 mm with the application of high pressure coolant (Hirosaki et al., 2004). The tool life of a BCBN tool increases with the increase of cutting speed during milling of Ti-6Al-4V when depth of cut is constant and feed rate is low (0.075 mm/rev) (Wang et al., 2005a). During machining workpiece material attaches to the flank face of the BCBN tool and tends to protect the tool from wear; albeit for a short time. The attached workpiece material as well as particles of tool material is removed with subsequent machining and the consequence is an accelerated attrition wear on the flank face. Non-uniform wear in the flank is the dominant wear pattern for BCBN tool during machining Ti-6Al-4V. There evidence of diffusion-dissolution wear and attachment of workpiece material to the rake face, but these are not main causes of tool failure (wang et al., 2005a and 2005b)

Some coatings, such as, TiN (by physical vapour deposition) and TiCN + Al_2O_3 (by chemical vapour deposition) are shown to improve life of carbide tools (milling process) at high performance milling process (speed 55 m/min with radial depth-of-cut to tool diameter

ration 72.5%) (Jawaid et al., 2000). Both of these two cutting tool materials exhibit a tool life of 30 min (with radial depth-of-cut to tool diameter ration 72.5%) at the cutting speed of 55 m/min and a feed of 0.1 mm per tooth. TiCN (3.1µm) and AlSiTiN (3.9 µm) coatings (by arc evaporation) also show better performances (almost double the tool life) at a cutting speed range of 50–130m/min (turning) in wet and minimum quantity lubrication (MQL) conditions, compared to the uncoated carbide tools. The nano-crystalline structure with the multilayer architecture, better abrasion resistance and superior adhesion properties of AlSiTiN coating produces enhanced performance - better than TiCN (Settineri and Faga, 2008). All coatings may not increase performance, such as, HfC coating. A six micron thick HfC coated tool was seen to wear (in the turning process) at about 20 times the rate of the identical uncoated tool (Turkovich et al., 1982). Carbide tools with a larger grain size (1.0 µm) demonstrate better resistance to flank wear due to lower solubility of WC in titanium alloys than those with smaller grain size (0.68µm) during dry turning of Ti-6246 (Jawaid et al., 2000).

The main causes of tool wear for different cutting tools are: coating delamination (coated tool), adhesion, attrition, diffusion, plastic deformation and cracks (Jawaid et al., 1999; Jawaid et al., 2000; Jianxin et al., 2008). A typical picture of cracks on coating during machining of titanium alloy is presented in Fig. 7. The coating delamination mainly occurs at the rake face at high speeds and feeds. It occurs as early as 10 second into machining for some coatings. Thus, there is doubt on the effectiveness of those coating. However, multilayered thick coating prolonged tool life as the multilayer coatings exhibit greater wear resistance and higher adhesion strength to the substrate (Ezugwua et al., 2003). The two possible reasons of coating delamination are (1) chemical reaction and (2) difference in the thermal expansion coefficient between the coating matrix and the substrate. Adhesion of workpiece material on cutting tool is very common during machining titanium. In some coated tools it takes place after the coating(s) has worn out/delaminated (Konig et al., 1991). With the progress of cutting, the welded (due to adhesion) work material on cutting tool is compressed and removed. This also leads to plucking of cutting tool grains which is called attrition wear. Attrition wear is observed on the rake face as well as flank face. Evidence of diffusion of cobalt and tungsten atoms into the work material has been reported when machining titanium with coated/uncoated carbide tools at reasonably higher cutting speed. The diffusion process, which is the main problem for machining titanium, comprises element diffusion and chemical reaction between the work piece and the tool. This type of wear is

more active at high cutting speeds or when there is a high temperature at the tool–chip interface, and is enhanced by a strong chemical affinity between the workpiece and the cutting tool materials (Molinari, 2002). The extreme temperature, pressure and the intimate contact at tool-chip interface offers a perfect condition for the diffusion of tool material to the workpiece (Jawaid et al., 2000). Ti, Al, and V of the Ti–6Al–4V alloy are seen to diffuse into the WC (Co binder) tools during machining at higher cutting temperature. Under similar conditions, W and Co of the WC (Co binder) tool also diffuse into Ti–6Al–4V alloy (Jawaid et al., 1999; Su et al., 2006). These change the composition and alter the performance of cutting tool (Jianxin et al., 2008). The diffusion of Co from the cutting tool weakens the bonding among carbide grains and thus with the progression of machining, attrition wear exposes Co from the underneath of the newly removed carbide particles. Due to high temperature and stress plastic deformation takes place at cutting edge during machining of titanium. Plastic deformation becomes more sever at higher cutting speed and feed. This is due to the higher cutting temperature and smaller contact at tool-chip interface at high cutting speeds as mention earlier. It is thought that in the region of the highest compressive stress the yield stress in the tool was reduced, which resulted in plastic deformation of the tool (Jawaid et al., 2000).

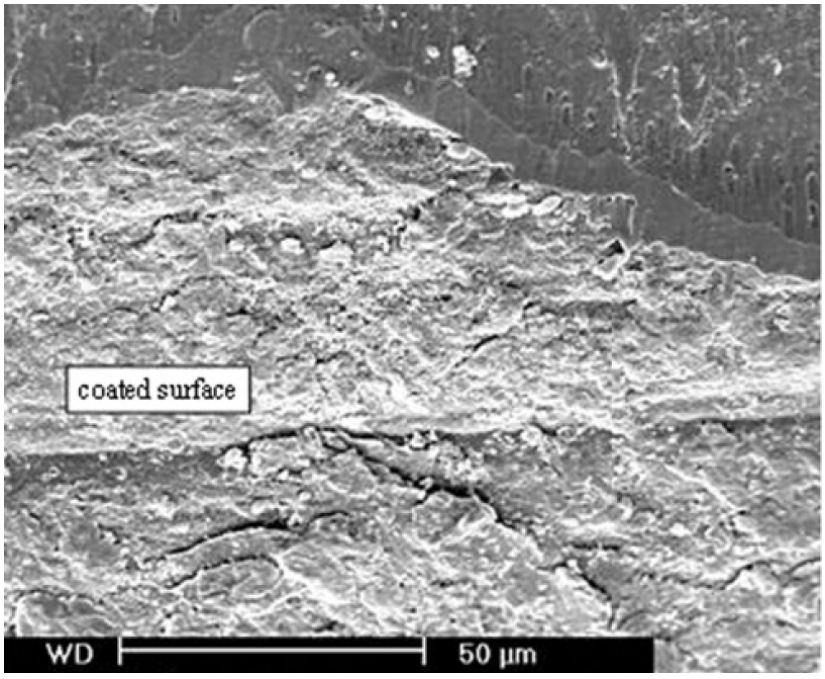

Fig. 7 Cracks in the coating layer at the leading cutting edge after machining at speed 100 m/min, feed 0.15m/min (Abdel-Aal et al., 2009).

Generally, several tool wear mechanisms take place simultaneously and those affect one another deteriorating and weakening the cutting tool and stimulating existing cracks to propagate. Among the above types of tool wear, diffusion and adhesive wear are the main mechanism to tool failure (Jianxin et al., 2008). Wears of carbide tools at different cutting conditions are presented in Fig. 6. According to (Jawaid et al., 1999) yield strength of the cutting tools reduces at higher cutting temperature and stresses generated on the flank face close to the tool nose which results in a greater wear rate at the nose area (Fig. 8). It shows that abrasion by carbide grains as a dominant wear mechanism (Dearnly et al., 1986, Hartung et al., 1982).

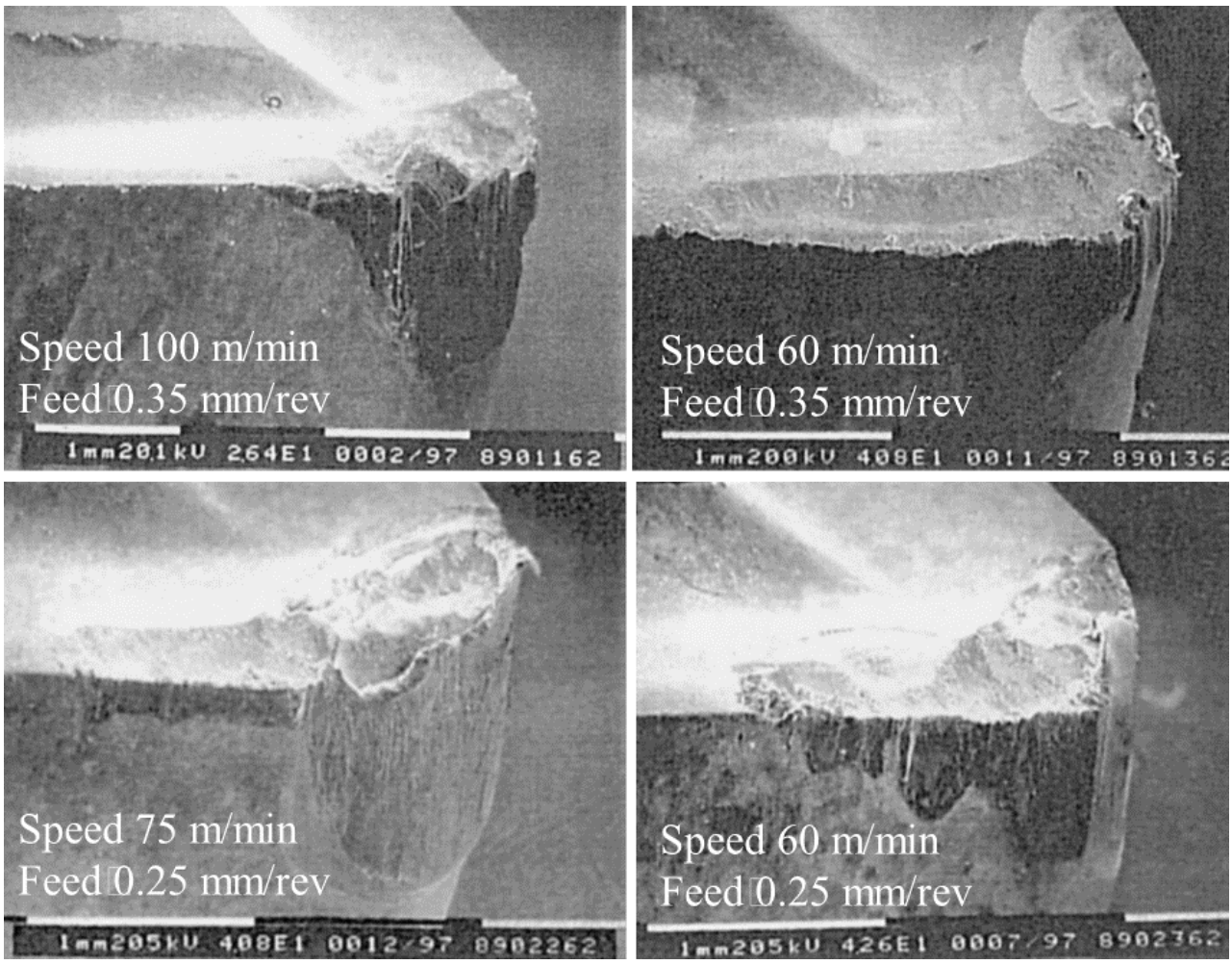

Fig. 8 Flank, rake and nose wear on tungsten carbide tool with 0.68µm grain and cobalt binder (Jawaid et al., 1999)

As discussed earlier, the cutting temperature is lower at lower machining speed and thus, the diffusion and chemical interactions between the carbide tool and titanium alloy is not

significant. At low machining speed, the tool wear is caused by mechanical fatigue as well as existing micro-fractures or defects in the tool. Cyclic mechanical and thermal stresses due to formation of saw-tooth chips mainly cause fatigue. Tool particles are easily plucked off from the cracked zone and these are often rubbed on the tool faces by chips resulting in abrasion wear. Abrasion is the major wear mechanism that causes of flank wear when machining with carbide tools at lower speed conditions (Dearnly and Grearson, 1986; Takeyama et al., 1983; Ezugwu et al., 2003).

(Turkovich et al., 1982) concluded that no tool materials show sufficient chemical stability for machining titanium to exhibit low wear rates due to low chemical solubilities in titanium. Thus, sliding between the tool and the chip needs to be eliminated to reduce wear. Due to adhesion a very thin layer of chip material forms on the tool face. This reduces the sliding between the tool and the chip, resulting in limited wear by diffusion of tool material through the adhered layer (Turkovich et al., 1982). The tungsten carbide based cutting tools form titanium carbide by chemical reaction with the titanium alloy, are commonly used to machine this material. The titanium carbide has high deformation resistance at cutting temperatures and adheres strongly to both the tool and the chip. Polycrystalline diamond which also forms TiC layer at the tool-chip interface shows better wear and deformation resistant than that of the tungsten carbide based cutting tools (Turkovich 1982).

Fig. 9 shows enlarged pictures of flank faces of two different carbide cutting tools. Smooth wear on the flank face is also noted underneath the adhered titanium on the flank face. The smooth wear pattern is due to the dissolution-diffusion wear mechanism. It seems that the dissolution-diffusion wears dominate on the flank face of the carbide inserts especially at high cutting speeds. Similar kind of wear is also noted in the rake face (Jawaid et al., 1999).

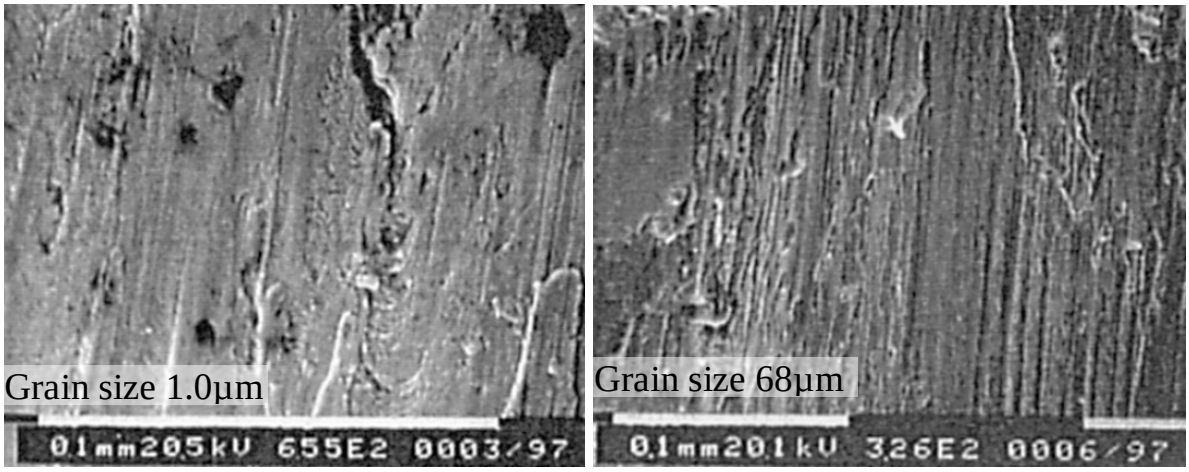

Fig. 9 Close-up view of the flank faces (Jawaid et al., 1999).

The theories (based on chemical dissolution of the tool material) to predict relative tool wear rate or tool wear do not work properly for machining titanium (Turkovich 1982). (Turkovich et al., 1982) carefully monitored the wear of polycrystalline diamond tools in turning of Ti 6A1-4V at 61.0 m/min. An adherent layer of titanium was seen on the rake face from the start of machining. After 15 minutes of cutting, 20 microns of wear was apparent on the rake face at different locations but there were regions with no wear. This kind of scallop wear on the rake face is also seen on the CBN and the coated carbide tools. Uncoated cemented tungsten carbide tools do not show this type of wear when machining Ti 6A1-4V, but a more conventional crater wear. Similar results i.e., smoothly worn area on rake and flank face of carbide inserts (94 wt.% tungsten carbide with 6 wt.% of cobalt binder) were noted while turning Ti-6246 titanium alloy. Abrasion wear mechanisms are seen to dominate the flank face and tool nose wear, and the maximum flank wear factor controls the tool life. Carbide tools with smaller grain size showed higher resistance to wear than that with larger grain size (Jawaid et al., 1999). Alloyed uncoated (W–Ti/Ta/Nb)C–Co and multi-layer CVD-coated (WC–Co)(TiCN/TiAlN/TiN) when end milling (radial depth of cut = 55% tool diameter, speed 100–125 m/min) of titanium alloy Ti-6242S under dry machining conditions showed acceptable tool life (5.82 to 21.2 min). Similar to other carbide tools, adhesion (attrition) and dissolution-diffusion are mechanisms of tool wear for these tools. The tool failure modes are plastic deformation and brittle fracture, such as, rake face flaking, cracking, chipping and fracturing (Haron et al., 2007). It was suggested (Turkovich et al., 1982) that this kind of wear pattern happens because of different interfacial conditions at different regions during chip generation. As mentioned earlier, a boundary layer of titanium forms at the tool-chip

interface and the relative motion between the tool and chip is controlled by shear within the titanium chip material. At certain cutting conditions titanium (Ti 6A1-4V) adheres to the tool and sliding does not take place at the tool-chip interface. Part of the boundary layer quickly becomes saturated with some tool material which limits the further diffusion of tool materials to chips. Thus, no wear occurs in certain regions on the rake face of some tools. The existence of TiC layer on the surface of the tool indicates the diffusion of carbon through the TiC layer. From this finding, (Turkovich et al., 1982) developed model to calculate tool wear rate based on the rate of diffusion of carbon through the TiC layer. The developed model predicted diamond and tungsten carbide tool wear rate accurately.

The number of research studies on machining, mainly turning and milling, of titanium is huge. Table 1 represent data for tool life and experimental conditions for turning and milling of titanium alloys based on the several important reports published in literature. It is noted that the variation of cutting parameters among the published papers is enormous. In many cases the details of machining parameters are not given properly. Therefor it is very difficult to compare different results and find out optimum machining parameters. Though these results do not provide exact prediction of machining outcomes, but try to address underlying mechanisms of machining and tool wear and predict trends of machining outcomes.

Table 1 Tool life and experimental conditions for turning and milling of titanium alloys

Table 1. Cutting tools, machining conditions and tool life for titanium alloys found in literature				
References	Cutting tool geometry and material: Diameter (mm) , angle (deg) edge radius (μm)	Cutting conditions: Speed (m/min) Depth of cut (mm) Feed (mm/per tooth)	Titanium alloy	Tool wear and life
	Milling process			

(Ginting and Nouari, 2006)	Ball-end milling: Diameter: 16 Rake angle: -6 Axial rake angle: -6 Radial rake angle:-2 Alloyed carbide: 69.8 wt% tungsten carbide and 9.5 wt% cobalt as a binder. Grain size 1–2 µm Hardness: 1485 HV_{10}	Speeds: 60–150 Axial depth of cut: 2.0 Radial depth of cut: 8.8 Feed rate: 0.1 and 0.15	Ti-6242S	Wear mode: flank wear and excessive chipping on the flank edge. Maximum tool life 22.4 min at 150m/min and 0.1mm/tooth
(Jawaid et al., 2000)	Diameter: 80 No. of inserts: 6 Approach angle: 45 Radial rake angle:-11 Axial rake angle:20 Effective rake angle: 6 (P25-P40, M30-M40, K20 - K30) PVD coated with TiN (M20-M30) CVD coated with TiCN+Al_2O_3 using	Speed: 55, 65, 80 and 100 Axial depth of cut: 2 Radial depth of cut:58 Feed: 0.1 and 0.15 Cutting fluid: Hocut 808, 6-7% concentration	Ti-6Al-4V	Wear mode: Coating delamination, attrition, diffusion and thermal cracks. Maximum tool life: 30 min for both inserts at 55m/min and 0.1mm/tooth Minimum tool life 5 min for both inserts at 100m/min and 0.15mm/tooth
(Haron et al., 2007)	Diameter: 16mm Cutting rake: −6 Axial rake:−6 Radial rake: −2 Alloyed uncoated carbide (W–Ti/Ta/Nb)C–Co Alloyed CVD-coated carbide (W–Ti/Ta/Nb)C–Co + (TiC+ TiCN + TiN)	Speed:100 to 125 Feed: 0.15–0.20 Axial depth of cut: 2–2.5 Radial depth of cut: 8.8 Dry machining	Ti-6242S	Wear mode: adhesion (attrition) and dissolution-diffusion. Plastic deformation and brittle fracture. Tool life: 5.82 to 21.2 min at cutting speeds:100–125 m/min
(Nouari and Ginting, 2006)	Nominal diameter: 16 Cutting rake:–6, Axial rake –6 and Radial rake: –2. Uncoated carbide tool and multi-layer (TiN, TiCN and TiC) CVD-coated tool	Speeds: 100 to 125 Feed: 0.15 to 0.20 Axial depth of cut: 2 to 2.5. Radial depth of cut: 8.8 Dry machining	Ti-6242S	Wear mode: Adhesion wear (attrition and galling) and diffusion wear. Coating delamination plastic deformation Tool life: 6-13min at speed 100-110 m/min

(Yasir et al., 2009)	Nominal diameter: 16 Insert diameter of : 10 Cutting rake: −4 Axial rake:+6 Radial rake −4 PVD coated cemented carbide tools	Speed: 120, 135 and 150 Depth of cut: 2 and 2.5 Feed: 0.1 and 0.125 Dry and near dry (or MQL) machining with coolant flow rate of 50 and 100 mL/H	Ti-6Al-4V	Maximum tool life was 8.5 min at Speed: 120m/min, depth of cut: 2mm and feed: 0.1 mm/tooth at dry condition.
(Su et al., 2006)	Cutting tool: Walter ZDGT150420R, TiN/TiC/ TiN coated carbide, one tooth	Speed: 400 Feed: 0.1 Axial depth of cut: 5.0 Radial depth of cut: 1.0 Case 1: Dry; case 2: flood coolant; case 3: nitrogen-oil-mist; case 4: compressed cold nitrogen gas (0, −10 °C); case 5: compressed cold nitrogen gas and oil mist (−10 °C)	Ti-6Al-4V	Wear mode: coating delamination, adhesion, diffusion and thermal crack. Tool life: 3.639, 5.081, 5.107, 7.195, and 9.792 min for Cases: 1, 2, 3, 4 and 5 respectively
(wang et al., 2005a)	Binderless cubic boron nitride (BCBN). Clearance angle: 20 Axial rake: 1 Radial rake: 10 Number of tooth: 1 Cutter diameter: 20 Milling type slot milling	Speed: 300, 350, 400 Depth of cut: 0.05, 0.075, 0.1 Feed rate: 0.05, 0.075, 0.1 Cutting fluid: high pressure coolant	Ti-6Al-4V	Wear mode: Abrasion, attrition and diffusion–dissolution wear. Non-uniform flank wear. Maximum tool life was 39.8 min at speed 400, feed 0.075 and depth of cut 0.075. Minimum tool life was 1.37 min at speed 400, feed 0.125 and depth of cut 0.125.

(wang et al., 2005b)	Binderless cubic boron nitride (BCBN). Clearance angle: 20 Axial rake: 1 Radial rake: 10 Number of tooth: 1 Cutter diameter: 20 Milling type Slot milling	Speed: 350 Depth of cut: 0.05, 0.075, 0.1 Feed rate: 0.05, 0.075, 0.1 Cutting fluid High pressure coolant	Ti-6Al-4V	Wear mode: Abrasion, attrition and diffusion–dissolution wear. Non-uniform flank wear. the tool life is about 20 min when milling Ti–6Al–4V with a cutting speed, 350 m/min; a feed rate, 0.05 mm/tooth; and a depth of cut, 0.075 mm; while at the same cutting condition, the tool life of CBN tools is only about 1 min
	<u>Turning processes</u>			
(Jawaid et al., 1999)	SECO Tools: CNMG 120408-890, CNMG 120408-883 Both inserts consisted of 94 wt.% tungsten carbide with 6 wt.% of cobalt as binder	Depth of cut: 2 Feed rates: 0.25 and 0.35mm/per rev. Cutting speeds: 60, 75 and 100.	Ti-6246	Wear mode: dissolution, diffusion, attrition and abrasion Maximum tool life: 11min at 60m/min and 0.25mm/rev. Minimum tool life was few seconds at 100m/min
(Nandy et al., 2009)	Insert geometry in orthogonal rake system: inclination angle -6°, orthogonal rake -6°, orthogonal clearance of the principal flank 6°, auxiliary orthogonal clearance 6°, auxiliary cutting angle 15°, principal cutting edge angle 75°, nose radius 0.80mm, edge radius 33µm. Uncoated microcrystalline ISO grade K20 inserts.	Depth of cut: 2 Feed 0.16, 0.20 and 0.24 mm/rev Cutting speeds: 90, 100 and 111. Cutting fluid: conventional wet and high- pressure neat oil and high-pressure water-soluble oil.	Ti-6Al-4V	Wear mode: adheso-diffusive wear, thermo-mechanical shock and plastic deformation. Maximum tool life: 28.65 with high pressure (140 bar) water soluble oil at 90m/min and 0.16mm/rev.
(Machado et al., 1998)	Straight grade (K20) cemented carbide inserts	Speed: 62, 75 and 84 Feed: 0.25 and 0.07 mm/rev depth-of-cut 2.5 mm High pressure (14.5 MPa) water based coolant (4% concentration)	Ti-6Al-4V	Wear mode: diffusion and fracture Maximum tool life: 32min at 62m/min and 0.25mm/rev with high pressure coolant.

(Zareena and Veldhuis, 2012)	Uncoated and perfluoropolyether polymer coated diamond tools. Ultra-precision turning Rake angle: 0 Clearance angle: 5 and 7.5 Nose radius: 0.3, 0.5 and 1.5 cutting edge radius range 60-130 nm	A fine mist of high purity canola oil. Speed 60m/min, Feed 1.5µm/rev, Depth of cut: 2 µm	Commercial pure titanium and Ti-6Al-4V	Wear mode: graphitization and adhesion. Coating delayed the wear.
(Haron, 2001)	uncoated cemented carbide tools ISO designation CNMG 120408	Cutting speed: 100, 75, 60 and 45, Feed: 0.35 and 0.25 mm/rev, Depth of cut: 2.0 mm	Ti-6Al-2Sn-4Zr-6Mo	Wear mode: flank face wear and excessive chipping on the flank edge, diffusion, abrasion, attrition, chipping, and plastic deformation Maximum tool life: 11min at 60m/min and 0.25mm/rev. Minimum tool life was few seconds at 100m/min
(Ezugwu et al., 2005)	Cubic Nitride Boron (CBN) Uncoated carbide tools Approach angle: 95°, back rake angle:–6°, end relief angle: 6°, side rake angle: –6°, side relief angle: 6°.	Cutting speed: 150, 200 and 250. Depth of cut: 0.5 Feed rate: 0.15 Hocut 3380 at a concentration of 6% Conventional as well as high pressure	Ti-6A-4V	Maximum tool life of around 4min for CBN tool at 150m/min with coolant pressure of 20.3MPa. For carbide tool it is around 5.7min at 150m/min with coolant pressure of 11MPa.

(Ezugwu, 2007)	PCD inserts Approach angle: 95°, back rake angle:–6°, end relief angle: 6°, side rake angle: –6°, side relief angle: 6°.	Cutting speed: 175, 200, 230 and 250 Depth of cut: 0.5 and Feed: 0.15 A high lubricity emulsion coolant containing alkanolamine salts of fatty acids and dicyclohexylamine applied at a concentration of 6%.	Ti-6Al-4V	PCD inserts under conventional coolant flow (feed: 0.15 mm/rev): 5.4min tool life at 175m/min and 3min at 200 m/min. But under similar conditions the tool life improved to 63.8min and 37.4min respectively with 11MPa of coolant pressure. With the further increase of coolant pressure to 20.3 MPa the tool life improved to 115.5 and 50.5min respectively
(Nabhani, 2001)	PCBN (AMBORITE*), PCD (SYNDITE) and TiC/TiC-N/TiN coated tungsten carbide tool	Cutting speed: 75 Feed: 0.25 Depth of cut: 1.0 Dry machining	Ti-6Al-4V	Wear mode: dissolution-diffusion process. Tool life for PCD, PCBN and Carbide tools are: 37.5, 15 and 8mins respectively.
(Venugopal et al., 2007)	uncoated microcrystalline grade carbide Insert geometry in orthogonal rake system: inclination angle -6°, orthogonal rake -6°, orthogonal clearance of the principal flank 6°, auxiliary orthogonal clearance 6°, auxiliary cutting angle 15°, principal cutting edge angle 75°, nose radius 0.80mm,	cutting speeds: 70, 100 and 117 Feed: 0.20 Depth of cut: 2.0mm Dry, wet and cryogenic cooling	Ti-6Al-4V	Wear mode: adhesion–dissolution–diffusion wear, attrition, micro and macro fracturing of the cutting edge and depression of the cutting edge. Maximum tool life: 7 14 and 24 min under dry, wet and liquid nitrogen cooling at cutting speed: 70 m/min.

(Settineri and Faga, 2008)	AlSiTiN and TiCN coated (by PVD) and uncoated WC-Co tool inserts (SPGN090308).	Speed: 50, 90, 130 Feed: 0.25mm/rev Depth of cut: 1mm Dry, wet and MQL turning	Ti-6Al-4V	Wear mode: delamination, fatigue cracks in coating, Maximum tool life: 7.4 min for AlSiTiN coated tool at 50m/min with MQL.

Form the above table it is clear that different researchers used different tools, cutting conditions and alloys, and obtain results. In addition, in many cases details of experimental processes are also missing. Thus, systematic quantitative comparisons among different studies are almost impossible. However, the results given in the table 1 are certainly valuable qualitatively. It shows that all cutting tools during machining titanium experience similar kind of problems and tool wear increase significantly with the increase of speed.

Undercut and distorted machined parts

Highly elastic workpiece material has the tendency to move away from the cutting tool at the point of machining. But it moves back after the cutting tool is passed during machining. This result in undercut of the parts and produces parts bigger than expectation. The tendency to move away of titanium alloy workpiece from the cutting tool causes dimensional error of the machined parts. Fig. 10 shows the typical effect of spring back during machining. It is found that the magnitude and directions of resultant forces are affected by the radius of the cutting edge, the flank angle, and the springback depth. (Islam et al., 2013) investigated the dimensional error of a titanium part during turning. It was noted that for a cylindrical bar of 45mm nominal diameter the error was as high as +0.23 mm. Similarly for the same cylindrical bar the circularity was 5.12 µm.

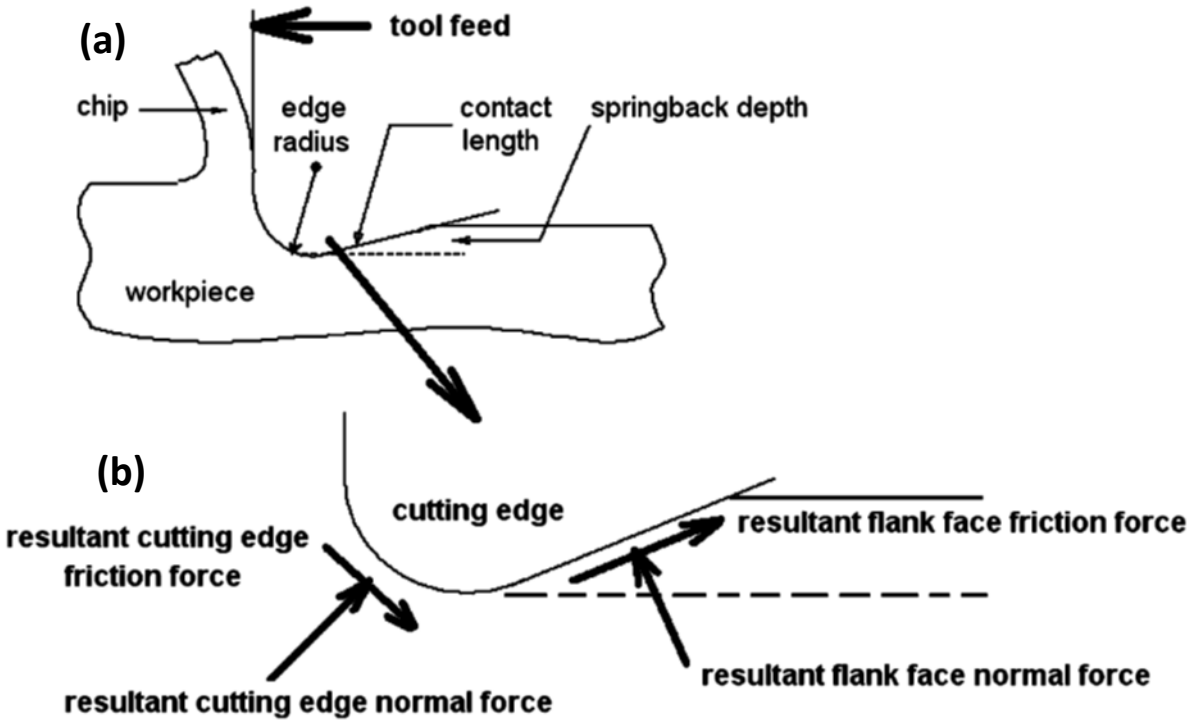

Fig. 10 Effects of springback, tool cutting edge and flank on the magnitude and directions of the resultant forces (a) bigger view and (b) magnified view of the cutting edge region (Friedrich and Kulkarni 2004).

According to (Friedrich and Kulkarni, 2004), the springback in milling process is a linear function of tool edge radius and the ratio of material hardness to elastic modulus. It can be expressed using the following equation: $s = kr\frac{H}{E}$, where s is springback, k (≈ 43) is a constant, r is cutting edge radius, H and E are hardness and Young's modulus of the workpiece material respectively. Significantly, low Young's modulus and reasonably high hardness/yield stress make titanium alloy highly elastic which can cause excessive workpiece deflection and small plastic deformation. Thus, it springs back i.e. there is a bouncing action as the cutting edge enters the cut during machining processes under cutting pressure (Campbell, 2006). This also leads to a lower effective clearance angle at the flank face, enhanced friction and chatter. Besides high cutting forces the low excitation frequencies, caused by relatively low rotation speeds, propagate chatter (Abele and Fröhlich, 2008). This reinforces the chatter generated due to high local temperature and saw-tooth chips. The normal contact stress due to springback can be written as, $= k_2 H \frac{s^2}{k^2 r^2}$, where k_2 (≈ 4.1) is a constant (Friedrich and Kulkarni 2004). The normal contact stresses arises in too-chip and

tool-workpiece interfaces which act normal to the cutting tool surface. All these lead to cyclic high stress on cutting tool.

The distortions of machined parts occur due to release of the inherent residual stress as the material is removed layer by layer during machining process. The distortion of parts happens very often during machining of aerospace parts made of titanium as the aerospace components are predominantly manufactured from large stock material by removing huge amounts of material to reduce the number of joints in the parts and make the structure stronger. Sometimes the weight ratio of stock material to final product becomes more than 50. The main reason of residual stress is the difficulty of uniform cooling large stock material casting. Cooling process takes place layer by layer. The outer layer solidifies and cools down to room temperature first. Due to the solidification and reduction of temperature the outer layers shrinks and apply compressive pressure to the internal materials which is hot and soft. These causes mismatch in the structure of the materials and residual stresses are generated in the titanium alloy casts. The low thermal conductivity may be a factor that inversely affects the cooling process. Thus, proper cooling rate and cooling methods need to be maintained to minimize the internal residual stress. The different heat treatments of the cast may improve the quality but large titanium blocks without residual stress is very difficult to achieve. At the start of the machining process of a big cast, the residual stress starts to release and the machined part starts to distort. This problem becomes critical when the weight ratio of stock material to final product becomes higher and, unacceptable if the stock material is embedded with very high residual stress (Pramanik, 2014).

IMPROVEMENT OF MACHINABILITY OF Ti-6Al-4V

To improve the machinability of titanium alloy some techniques need to be considered to avoid saw-tooth chip formation, high temperature and high stress. However, all of these cannot be eliminated at a time with any technique. There are several techniques that can reduce or adjust the unwanted phenomenon during machining titanium alloy. The following section describes all the available techniques and their working principles and suitability.

Low speed machining

Saw-tooth and high temperature generation can be avoided if titanium alloy is machined at low cutting speed. The critical cutting speed for the onset of segmented chip depends on the microstructure. (Sun et al., 2009) obtained saw-tooth chips as well as continuous chips (Fig. 11) during machining titanium alloy at speed 16m/min (very low), depth of cut 1.5 mm and feed 0.28 mm/rev.

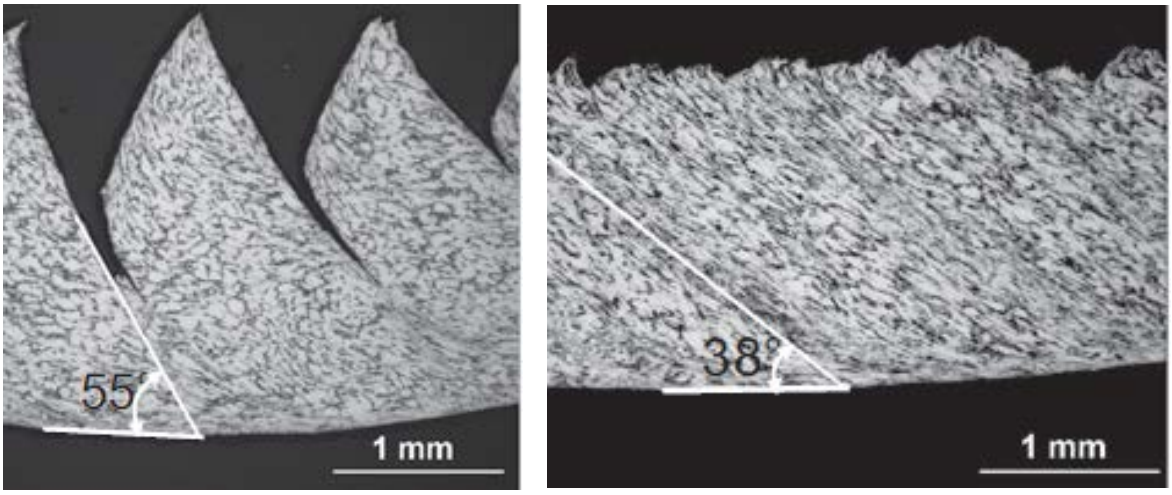

Fig. 11 Segmented and continuous chips from same workpice at similar cutting condition (Sun et al., 2009).

This is due to the inhomogeneous structure of the workpiece material, some areas would exhibit good plastic deformability at low cutting speed, resulting in continuous chip formation (Fig. 11) and static cutting forces. However, other areas show poor plastic deformability is unable to deform at this cutting speed. Therefore, results in saw-tooth and dynamic cutting forces. The traditional approach of machining titanium is to use low cutting speeds, high feed rates, higher depth of cut and use ample amounts of cutting fluid. In addition, machine tools should be vibration free and cutting tools should be sharp and replaced at the first signs of wear (Campbell, 2006). Though the higher depth of cut has the tendency to unstabilize the machining process, at lower speed the machining process falls in the processes dampening zone even when depth of cut is larger.This has been further clarified in the next section. But the low speed machining process is no more economical as much machining time is spent on finishing processes. Several finish cuts for titanium alloy parts are highly desired because of tendency of spring back, residual stress and saw tooth chip. Thus, there are several other methods to improve the productivity of titanium machining as

described below. Machining of any material at low speed is neither economical nor acceptable as it reduces the productivity by increasing the machining time.

Application of vibration analysis kit

High speed machining technology is quite old but the application of vibration analysis technology in high speed machining has been getting popular in machining of difficult to cut materials, such as titanium, in recent years. In titanium milling, surface speed and radial depth of cut are the two key variables that govern tool life and they are interlinked. In practical machining operation maintaining uniform radial depth of cut is extremely difficult. If radial depth of cut can be accurately controlled within the tool path the surface speed and axial depth of cut can be increased. Cutting tools normally chatter at relatively higher cutting speeds. These speeds may be in the acceptable range for a cutting tool to machine titanium alloys. Here the acceptable range of speed indicates the speed at which the tool wear rate is reasonably acceptable. Commonly accepted surface speed limits for a carbide tool are: (a) 100- 220 m/min for up to 25% radial immersion (b) 55-90 m/min for up to 50% radial immersion and (c) 40-60 m/min for 50%-100% radial immersion (Pramanik, 2014). If chatter occurs at the lower end of the above speed range then significant gains in machining time can be made by combining dynamic analysis with controlled tool paths and knowledge of the upper limits of the achievable surface speeds, axial depth of cut and radial depths of cut.

No machining system is perfectly rigid. Thus the vibration is always present between the tool and the workpiece in machining process. In case of machining titanium alloys, the vibration becomes more susceptible to occur due to self-excited vibration between the workpiece and the cutting tool. Localized shearing which is associated with the generation of cyclic forces is responsible for self-excited vibration (Fan et al., 2011). This vibration causes waviness of the surface in the first cut. In the following cut, the tool cuts into the wavy surface which causes further variation of chip thickness and force that excites the structure, producing greater vibration between the tool and the workpiece. This is called “waviness regeneration.” The vibration may grow after each subsequent pass, if tool vibration and surface waviness are not in phase and the process becomes unstable. The chip thickness variation is negligible and there is no appreciable force variation when the wavy surfaces between two revolutions (cutting passes) are in phase. This permits stable cutting with large chip widths. Considering

that tool vibrates in at its natural frequency, it is natural that matching the workpiece rotating frequency (spindle speed) to the tool's natural frequency will lead to this preferred "in phase" situation (Schmitz and Smith, 2008). The gain in variation of force and chip thickness depends on the axial depth of cut and speed. If the axial depth of cut is doubled the gain becomes double in an unstable machining process. The process is always stable with small depth of cuts. Chatter will eventually be encountered if the depth of cut is increased (Leigh et al., 2000) and it occurs at certain combinations of axial depth of cut and spindle speed.

To define the stable machining condition a frequency response function (FRF) for a machining system needs to be established. A frequency response function expresses the structural response to an applied force as a function of frequency. The response may be given in terms of displacement, velocity, or acceleration. Furthermore, the response parameter may appear in the numerator or denominator of the transfer function (*http://www.cs.wright.edu/~jslater/SDTCOutreachWebsite/intro_freq_resp_functions.pdf*).
The basic hardware required to measure FRFs are (a) a mechanism for known force input across the desired frequency range, (b) a transducer with the required bandwidth for vibration measurement, and (c) a dynamic signal analyzer to record the time-domain force and vibration inputs and convert these into the desired FRF. The dynamic signal analyzer includes input channels for the time-domain force and vibration signals and computes the Fourier transform of these signals to convert them to the frequency-domain. It then calculates the ratio of the frequency-domain vibration signal to the frequency-domain force signal; this ratio is the FRF. The FRF is then analysed to plot stability lobe diagrams (Schmitz and Smith, 2008). Stability lobe diagram is a plot of axial depth of cut vs. spindle speed where the chatter free machining conditions are clearly defined. There are several companies that commercially sell vibration analysis kit.

A typical stability lobe diagram is given in Fig. 12. This plotting varies machine to machine which indicates that no two machines are dynamically similar. For a particular machine the cutting conditions in red-shaded areas are not stable. Chatter by heavy vibration, tool damage, poor surface quality and scrapped workpieces occur when the cutting parameters are in the red shaded area. On the other hand, the machining conditions in the white areas will be stable, producing no chatter.

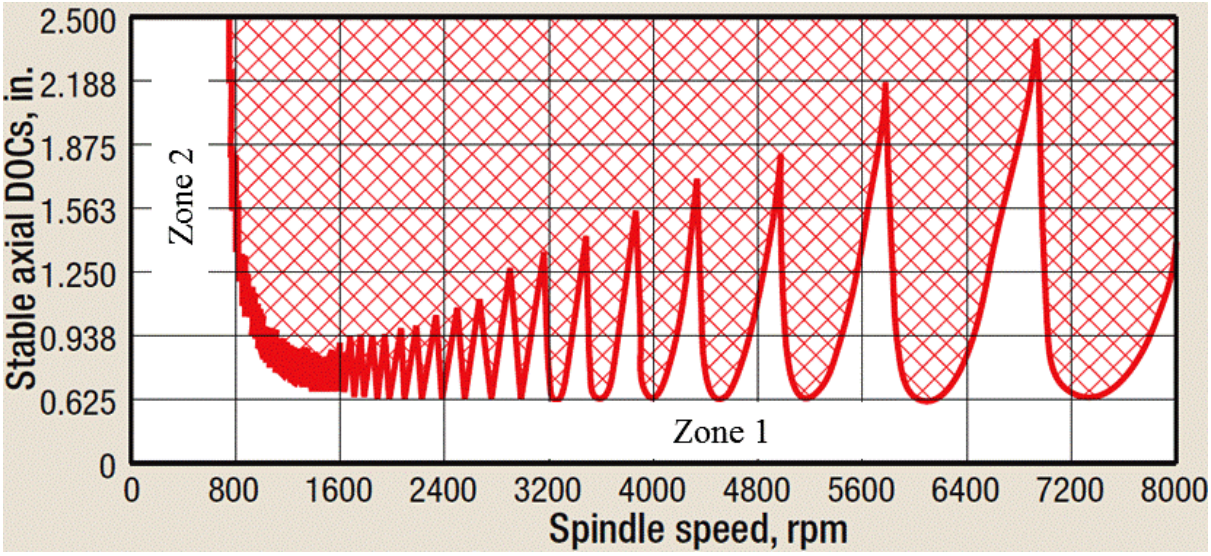

Fig. 12 A typical stability lobe diagram (*http://www.mfg-labs.com/FileDownload/Papers_Presentations/CTE_May2009_ss.pdf*)

According to this figure, a larger axial depth of cut can be applied if the spindle speed is low. In this case, the low spindle speed is less than 800 rpm. With the increase of spindle speed the depth of cut needs to be reduced to have stable machining. For example, if spindle speed is 1600 rpm the depth of cut should be around 0.625 in or less to avoid chatter during machining. With the further increase of the spindle speed, the permissible axial depth of cut increases again, but only in specific spindle speed ranges where stable pockets are exists. For example, there are large, stable pockets around 4,800 to 4,900 rpm, around 5,600 to 5,700 rpm and around 6,700 to 6,800 rpm where the axial depth of cut can around 1.35, 1.57 and 1.95 respectively. (*http://www.mfg- labs.com/ FileDownload/ Papers_ Presentations/ CTE_ May2009 _ss.pdf*). Therefore, this method can increase the speed as well as depth of cut significant. If the depth of cut is increased to double, which is easily possible, the material removal will be doubled as well.

The milling of titanium alloy is typically restricted to areas 1 and 2 (Fig. 12) due to poor tool life at high surface speeds. Zone 1 can be optimised through control of radial depth of cut and Zone 3 could be controlled to extend to useful surface speed range which is known as process damping. The process damping inhibits chatter vibrations at low speeds by damping force which is caused by interference between the relief face of the tool and the machined surface. It is influenced by chip thickness and tool geometry. The indentation of material under the flank face of the tool generates a great source of damping (Wu, 1989; Chiou and

Liang, 1998). (Huang and Wang, 2007) noted that the indentation of material, among the different sources of process damping, dissipates biggest portion of vibration energy at low cutting speed. (Ahmadi and Ismail, 2012) integrated equivalent viscous model of process damping into the multi-frequency solution and the semi-discretization method to establish the stability lobes in milling. The performance of these two methods was conducted by time domain simulations. It was noted that higher harmonics are needed at low speed cuts and highly damped systems. Higher stability arises at low speeds in highly damped systems with no process damping (Ahmadi and Ismail, 2012).

Thermally enhanced machining

Thermally enhanced machining process uses precise coordination between the cutting tool and a heating source to raise the metal surface temperature in the path of the cutting tool so that it can be removed more easily. Thermally enhanced machining process uses an external controlled heat source, such as laser heating, to heat and soften the workpiece material ahead of the machining point. Thus, thermal softening occurs not only at the machining point but in a wider zone. With the increase of temperature the strength of materials normally decrease due to thermal softening, thus the reduction cutting forces. In addition, the rate of strain hardening also decreases at higher temperature. Therefore, the thermally enhanced machining process has strong potential in machining the hard-to-machine materials, such as, titanium. The hexagonal closed pack atomic structure of Titanium (Ding et al., 2012) contributes to deform differently at high temperature and strain rate as deformation twinning is also effective in titanium. The deformation substructure of Ti-6Al-4V consist of planar slip in the α grains at quasistatic strain rates. Deformation twinning is observed in addition to planar slip at higher strain rates (3000 s^{-1}). The temperature around 495 K alters the deformation mode to more random slip (Follansbee and Gray, 1989). At higher temperatures the strain hardening recovers the normal trend of decreasing with increasing temperature and decreasing to almost zero at 600°C. This variation in hardening is considered to be the result of dynamic recovery happening at the intermediate temperatures at low deformation rates. On the other hand, the high rate data shows a strain hardening rate decreases almost monotonically from 200 to 734°C. A slight change in the strain hardening rate is noted between 250 and 600°C above 10% strain, but the change is much smaller than that observed at low strain rates (Lennon and Ramesh, 2004). Thus the presence of the recovery and twinning mechanisms considerably

complicates the deformation mechanism of titanium. For the same reason, the selection of proper heating temperature and machining condition during thermally enhanced machining is very important. Fig. 13 shows the cross section of a chip produced by laser assisted machining at the cutting speed 150 m/min and laser power of 1900 W (Sun et al., 2010a). At this case continuous chips are produced even at speed as high as 150 m/min. This chip has a molten material layer of thickness 7.2 µm marked by A (Fig. 13) which was caused by the laser heating. There was a single martensite phase of 40µm thick as marked by B in the middle region. This was transformed from single beta phase. The bottom region of the chip which is marked by C consists of alpha and beta phases. The region C is refined by continuous shear deformation have 38° slipping angle which is equal to that of the conventionally machined chip at low cutting speed. Thus, the continuous chip produced at high cutting speed with thermal assistance seems to have comparable chip formation mechanism as that of a continuous chip formed at low cutting speed without thermal assistance (Sun et al., 2010a).

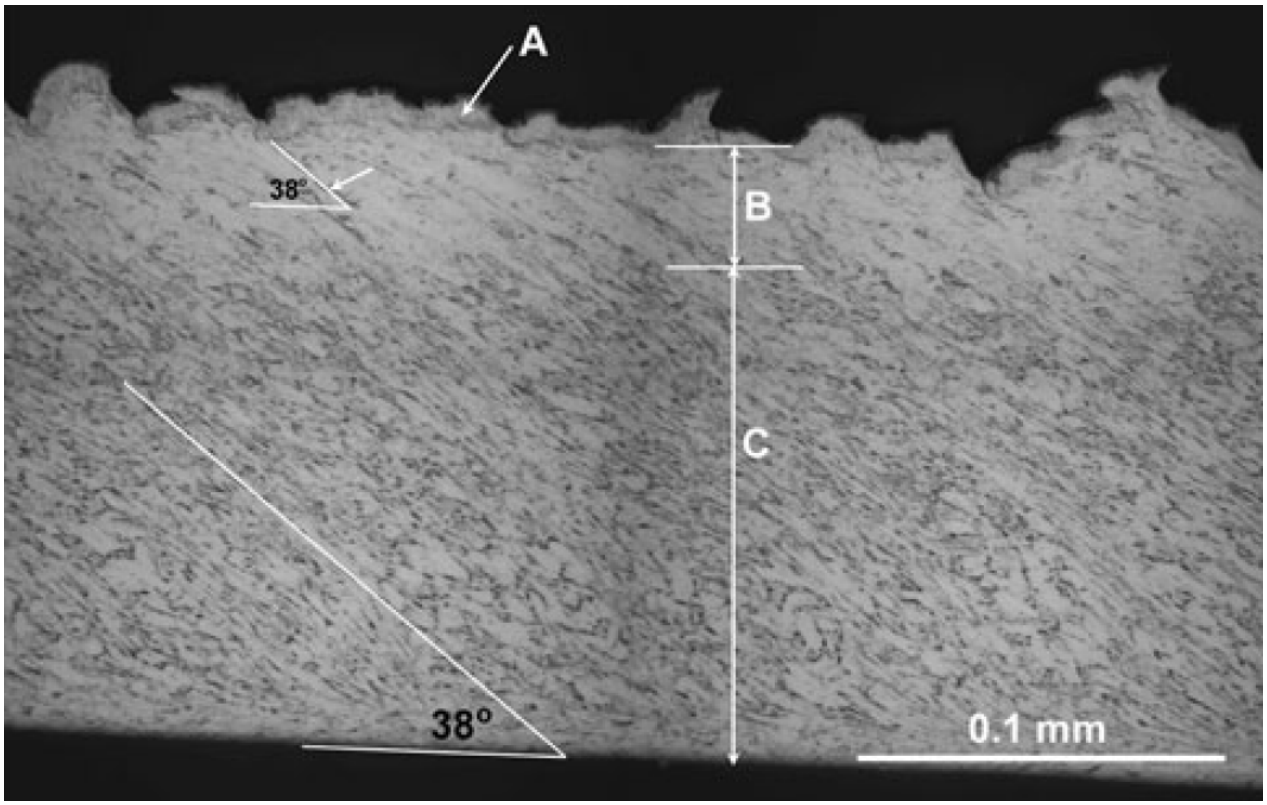

Fig. 13 Cross section of the continuous chip made by laser assistance at laser power 1900 W and cutting speed 150 m/min (Sun et al., 2010a).

The amount of the heat generated by plastic deformation and friction during machining on the workpiece surface temperature is negligible compare to the heat of laser, because of the small volume of the primary shear zone. But the effect of laser heating (properly controlled) on tool wear and surface quality is not significant as most of the heat is carried away by the chips. Laser beam heating in front of the cutting tool reduces the cutting forces as well as changes the material removal process. In laser assisted milling workpiece material is heated and softens before entering cutting zone. This heating and softening of the workpiece play a critical role in cutting force change, for example, the feed force reduces significantly with the increase temperature from 200°C to 450°C, but it does not continue to reduce with further increase of workpiece (Ti-6Al-4V) temperature. For this workpiece, feed force becomes much higher if the incident laser power melts the surface and phase transformation occurs (Sun et al., 2011). The chips produced by thermally enhanced machining are of much clearer edges, more uniform thickness, and smaller and homogenous segmentation. These result in smoother machined surface lower tool vibration (Sun et al., 2011). It shows that the critical cutting speed for the onset shear instability and chip segmentation increases with the localised preheating (Sun et al., 2010a). At a higher temperature the chip morphology transits from sharp saw-tooth morphology to a continuous chip but backs to a saw-tooth shape with further increase of the cutting speed. Laser heating improves deformability of material near the free surface which leads to the continuous chips. The critical cutting speed at which continuous chips are formed depends on the laser power, the surface temperature and the temperature gradient across the chip thickness in the cutting zone (Sun et al., 2010a). At and below the critical cutting speed (at certain temperature) the surface temperature and thickness of the molten and the single-phase material in the cutting zone enables the chips to deform steadily and completely. The critical cutting speed increases with heating temperature i.e., laser power (Sun et al., 2010a).

The high dynamic impact, mechanical and thermal fatigue, and adhesion of workpiece material on the cutting tool edge affect the tool life significantly during conventional milling of Ti-6Al-4V. Thermal softening of the workpiece by the laser beam in front of the cutting tool effectively reduces mechanical causes of tool wear, which reduces tool chipping. However, the temperature of laser heating, which depends on laser power and cutting conditions, needs to be very accurate in order to avoid overheating and degradation of the cutting tool. (Sun et al., 2011) achieved maximum tool life for milling of Ti-6Al-4V at

temperatures 230°C and 350°C approximately in front of the cutting tool with compressed air delivered through a stationary nozzle and the spindle respectively. The tool life with compressed air delivered through the spindle is much longer than that through a stationary nozzle at the optimum workpiece temperature. This is because of the better cooling of the tool and removal of chips from the cutting edge in the former case (Sun et al., 2011). At material removal temperature of 250°C reasonable tool life can be achieved at a cutting speed of 107 m/min during turning Ti-6Al-4V alloy (Dandekar et al., 2010).

Application of coolant

It is clear now that the efficiency of the titanium cutting process depends on the thermal/frictional conditions at the tool-chip interface. The use of coolant/lubricant improves the thermal/frictional conditions (Kovacevic et al., 1995). Thus, application of coolant is an integral part during machining of titanium alloy in machining industries. Coolant is more effective if it penetrates into the tool-chip and tool-workpiece interfaces during cutting process. This can drop the cutting temperature as much as 30% (Sun et al., 2010) and also acts like lubricant which leads to a longer tool life (Kitagawa et al., 1997; Palanisamy et al., 2009). The efficiency of the heat removal process depends on the heat transfer coefficient between the coolant and the cutting zone (Nandy et al., 2009). Flood cooling is commonly/conventionally applied to reduce heat and induce lubricant into the tool-chip and tool-workpiece interfaces (Bermingham et al., 2012). For high speed machining operations diluted solution of rust inhibitor and/or water soluble oil at 5–10% concentration can be used. On the other hand, chlorinated or sulfurized oils can be used for lower speeds and heavier cuts as these coolants minimize frictional forces which cause galling and seizing. Chlorinated oils may cause stress corrosion cracking if not cleaned properly (Campbell, 2006). At high cutting speed, the performance of conventional coolant techniques is limited due to inability to penetrate into the region adjacent to the cutting edge as coolants tend to vaporise at the high temperatures generated in the cutting zone (Ezugwu et al., 2003; Ezugwu, 2004).

To improve the effectiveness of cooling process, several technologies have been developed in recent years for controlling the temperature in the cutting zone in order to increase the overall effectiveness of the process like cryogenic cooling, solid coolants/lubricants, minimum quantity lubrication (MQL)/near dry machining (NDM), high pressure coolants (HPC), internal tool cooling and use of compressed air/gases (Sharma et al., 2009). Different cooling

methods have been tested during machining of titanium, such as, MQL, high pressure coolant, liquid nitrogen and cold air.

In high pressure coolant, the coolant pressure can be as high as 90 bar compare to conventional coolant pressure of 6 bar. Smaller chips are generally generated during turning of Ti-6Al-4V with the application of high pressure coolant directed into the tool-chip interface in the secondary shear zone. This is because the higher pressure creates a more effective chip removal process (Palanisamy et al., 2009). High pressure coolant can increase the tool life by almost 3 times mainly by reducing the machining temperature during turning Ti-6Al-4V material. The improvement of tool life is presented in Fig. 14. Under high pressure coolant, frequency of chip serration, shear-band thickness and average chip thickness increases. Thus chip morphology varies. The chip morphology and tool performance not only depend on pressure of coolant but also the coolant properties, such as, density, thermal conductivity, heat transfer coefficient and lubrication ability. These properties control the efficiency of cooling the cutting tool and chip breaking (by the momentum of coolant jet) process. The higher cooling rate and shorter chips provide longer tool life, lower machining forces and better surface finish. The better performance of water-soluble oil is found due to its higher momentum, thermal conductivity, heat transfer coefficient and lubrication ability compare to high-pressure neat oil (Nandy et al., 2009). The hardening effect on the machined surface is much lower when the high pressure coolant is used compare to that of conventional cooling. This is due to higher heat generation with conventional coolant supplies. Efficient cooling by high pressure coolant increases the access of the coolant to the machining zone. This reduces friction and heat generation which consequently lower temperatures and plastic flow. Thus, lesser hardening effect as well as micro-structural damage are generated when high pressure coolant is used (Ezugwu et al., 2007a).

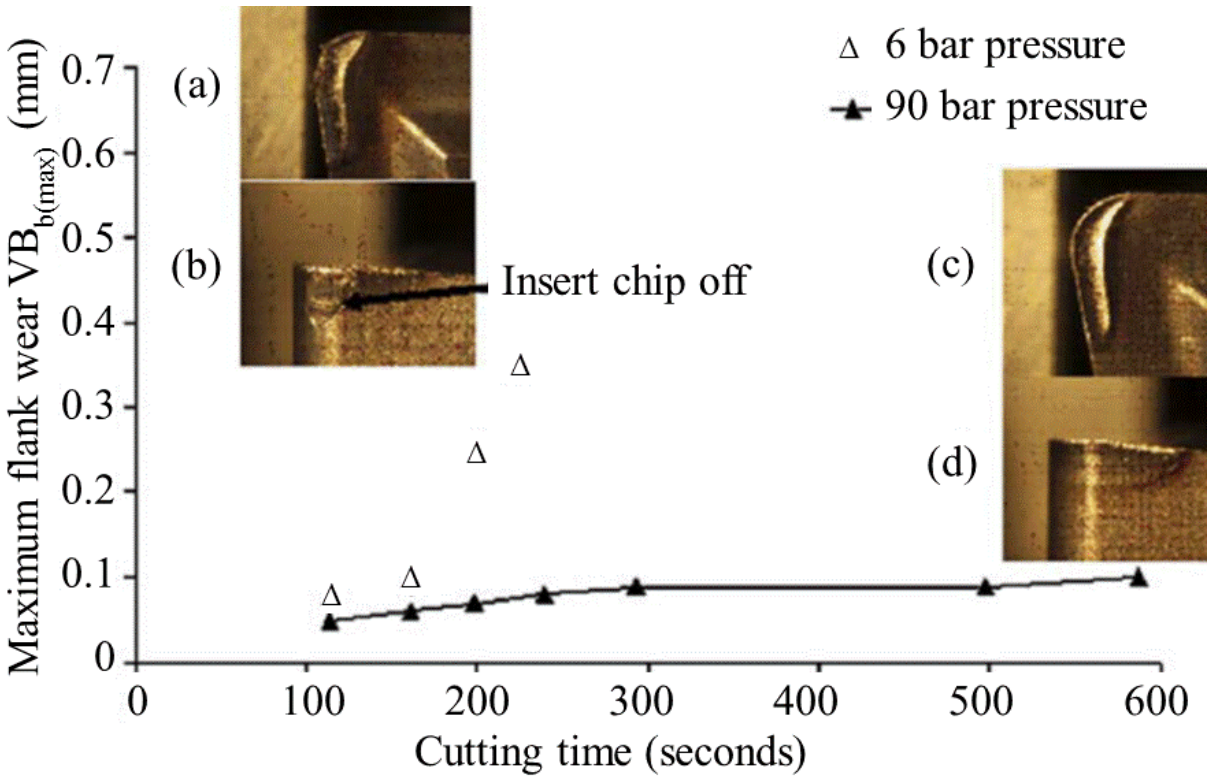

Fig. 14 Tool wear along with (a) and (c) crater view and (b) and (d)flank view of the insert obtained after tool chip-off with the application of standard and high pressure coolant (Palanisamy et al., 2009).

The factors influence the effectiveness of high pressure coolant include the material type, the depth of cut, cutting velocity, tool geometry and the position of the nozzle outlet (Bermingham et al., 2012). The nozzle outlet needs to be close to the cutting edge in case of the milling operations (Palanisamy et al., 2009a). Two methods can be used such as (1) coolant jet injected directly into the tool-chip interface through a hole in the tool rake face, and (2) coolant jet injected into tool-chip interface through an external nozzle (Kovacevic et al., 1995). High-pressure cooling was applied in machining of titanium alloys by (Kovacevic et al.,1995; Machado et al., 1998 and Lacalle et al., 2000). The researchers reported reduction in cutting temperature, cutting forces and coefficient of friction at the chip–tool interface along with improvement in tool life and productivity.

In cryogenic cooling, liquid nitrogen is most commonly used as a coolant. This type of coolant has received great interest recently because of the inherent environmental benefits, such as; nitrogen is a safe, clean, non-toxic fluid that evaporates into the atmosphere leaving no mess and requires no expensive disposal. Ice build-up on tools/tool holders and

unavailability of constant supply of liquid coolant are main disadvantages to this process (Bermingham et al., 2012). Cryogenic cooling with liquid nitrogen jets significantly extends the tool life by reducing the crater wear, flank wear and edge depression of the cutting tool insert during in turning of Ti-6Al-4V alloy. The reduction of tool defects is credited to lowering the machining temperature under cryogenic cooling (Venugopal et al., 2007). In addition, cryogenic machining reduces the cutting forces as well as coefficient of friction at the tool–workpiece interface (Strano et al., 2013). Under the application of this type of coolant the wear mechanisms, i.e., adhesion–dissolution–diffusion, remain unchanged. The extent of titanium alloy layer deposit on the crater surface is lesser under cryogenic cooling. The benefit of cryogenic cooling is substantial at moderate cutting velocity (Venugopal et al., 2007). The amount of heat removed from the cutting zone depends on the duration for which the heated area is in contact with the coolant. The cold air–chip interaction time becomes shorter at higher cutting speed. Thus the cooling efficiency reduces with the increase of cutting speed (Sun et al., 2010b).

(Hong and Ding, 2001) introduced dispense of liquid nitrogen through micro jets to the flank, the rake, or both near the cutting edge and investigated cutting temperatures at different cooling conditions. Temperatures in cryogenic machining were compared with conventional dry cutting and emulsion cooling. It was noted that a small amount of liquid nitrogen applied locally to the cutting edge is superior to application of emulsion. The study found that cooling approaches in order of effectiveness (worst to best) to be: dry cutting, cryogenic tool back cooling, emulsion cooling, precooling the workpiece, cryogenic flank cooling, cryogenic rake cooling, and simultaneous rake and flank cooling (Hong and Ding, 2001). (Dhananchezian and Kumar, 2011) modified the cutting tool insert by drilling holes so that liquid nitrogen can flow in the cutting zone for the efficient use of liquid nitrogen in the turning process. It was noted that cryogenic cooling by liquid nitrogen reduced the cutting temperature by 61–66%, cutting force by 35–42%, tool wear by 39% and surface roughness by 35% over wet machining.

(Sun et al., 2010b) took advantages of both the extremely low temperature of the liquid nitrogen and high pressure from the compressed air and developed new cooling approach. They applied liquid nitrogen cooled (cryogenic) compressed air to cool both the flank and rake faces of the tool. The effectiveness of this type of cooling is shown in the Fig. 15. Cryogenic air at high pressure can easily penetrate into the cutting edge to reduce the cutting

temperature and facilitate the chip removal by breaking. It was noted that the cryogenic compressed air show a significantly reduce the chip temperature but the cooling effect diminishes at higher cutting speed. The cooling effect is larger with a smaller feed than that with a larger feed at the same cutting speed (Sun et al., 2010b). In case of air cooling the heat from the cutting zone is removed by heat convection. The efficiency of heat removal depends on the convection heat-transfer coefficient and temperature of the coolant. The heat convection coefficient (≈2000 W/m^2 K) of air at high-pressure (4–7 bar) significantly increases over conventional dry air (≈20 W/m^2 K) (Bareggi et al., 2008; Kops and Arenson, 1999). Thus, better reduction of temperature by applying compressed air at the cutting zone. In addition, pressurized cooled air (by LN_2 at -196°C) further increases the heat removal rate and reduces chip temperatures. The cryogenic compressed air cooling affects the characteristics of the segmented chip and the transition from irregular to regular saw-tooth takes place (Sun et al., 2010).

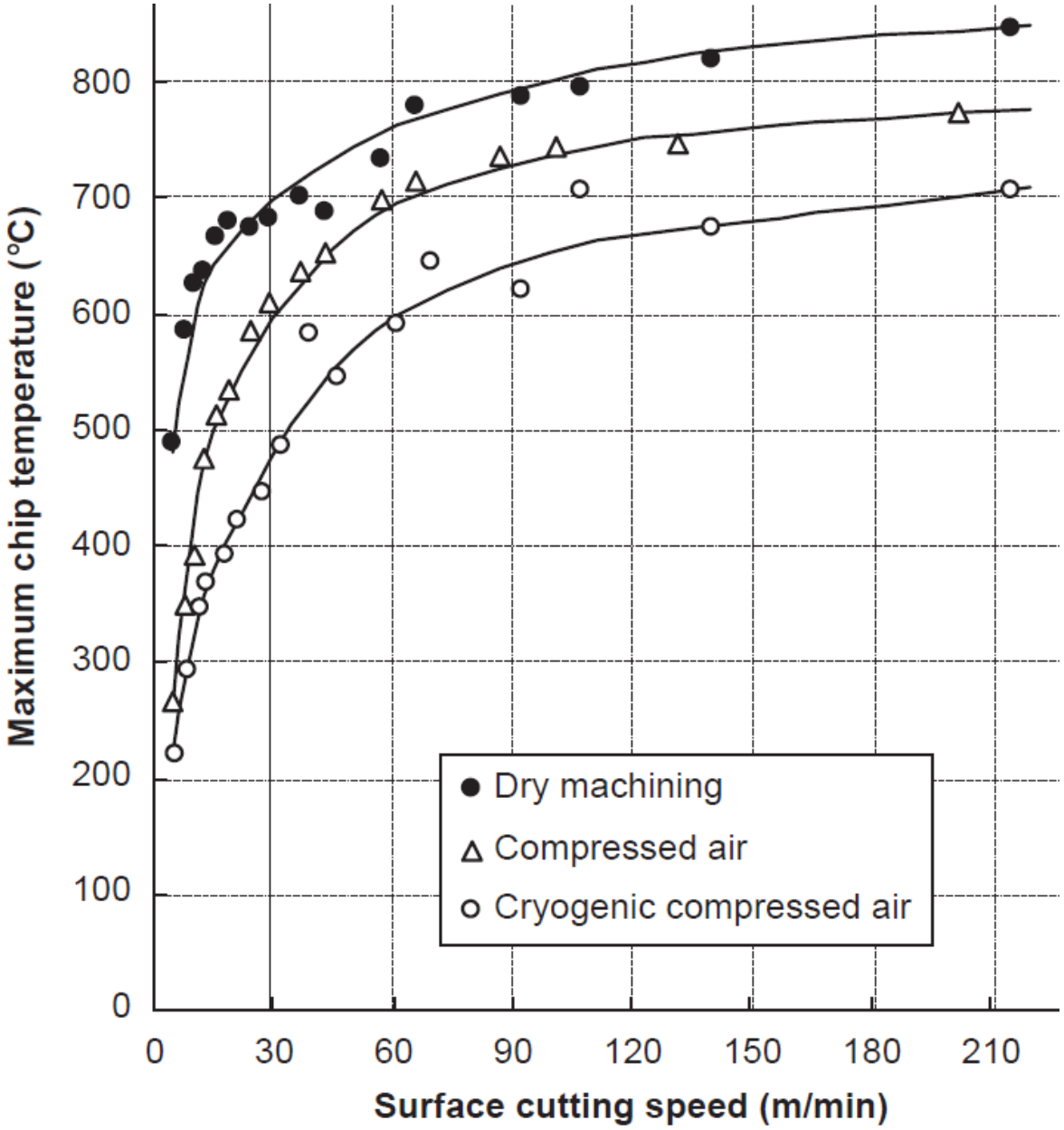

Fig. 15 Reduction of the maximum chip temperature with different cooling methods at feed 0.28mm/min (Sun et al., 2010b).

There are researches to eliminate or reduce the consumption of cutting fluid with the increased awareness of environmental and health issues. Minimal quantity lubrication (MQL) method can reduce cutting fluid consumption in machining process. In MQL technique, a small quantity of lubricant is dispensed to the tool–workpiece interface by compressed air flow internally/externally (Rahim and Sasahara, 2011; Coz et al., 2012). Very few researches on application MQL technique during machining of titanium alloy in the literature. Rahim and Sasahara, (2011) studied the drilling of Ti–6Al–4V under different cooling conditions to

understand the effectiveness of MQL compare to different lubricant types, such as, air blow and flood cooling. It was found that MQL technique gave comparable performance with the flood cooling condition. MQL technique with palm oil showed better performance than MQL technique with synthetic ester. But both of these reduced the workpiece adherence on the cutting tool compared to the dry condition. The cooling effect of MQL techniques is limited. Thus, consequently a significant rise in the temperature is noted in the tool and workpiece during the drilling process. Drilling temperature varies from 590 to 640 °C at cutting speed as low as 35 m/min with MQL. This temperature rise activates the tool wear mechanisms, reduces the tool life and affects the machining outcomes (Coz et al., 2012).

Cutting tool and tool holder

Higher heat generation is a big problem during machining titanium alloys due low thermal conductivity. The machinability can be improved if this heat can be removed from the cutting zone. In addition to the application of coolant, researchers used high conductive cutting tools to remove a significant amount of heat from the cutting zone. Takeyama et al., (1983) applied different types of cutting tools, such as, straight tungsten carbide tool, cemented TiN tool, pure aluminium oxide type of ceramic tool, TiC coated tool, CBN tool, sintered diamond tool and natural diamond tool for machining (turning) titanium alloy (Ti-6A1-4). The natural diamond tool which has highest thermal conductivity of all the tool materials available was used with abundant water-soluble coolant. This tool showed an excellent performance in machining titanium alloys at cutting speed as high as 200 m/min with abundant coolant. The surface machined with the natural diamond tool was better than those with the other (Takeyama et al., 1983).

The cutting heat can be dissipated efficiently by increasing the thermal conductivity of the tool shank. (Takeyama et al., 1983) designed a special tool shank with built-in large copper plate as a heat sink. The stability of the soldered part was tested when machining with the conventional tool shank and the improved tool shank at the cutting speed of 150 m/min. The flank wear width was only 0.03 mm after cutting half an hour with both tools. The damage of the soldering of the conventional tool shank was damaged and the diamond tip was changed. On the other hand, the tool tip is firmly fixed after a long time machining for the improved tool shank (Takeyama et al., 1983). In addition, round shaped cutting edges reduces crack

formation, increase strength and change load which lead to enhanced tool life (Rech et al., 2005; Bouzakis et al., 2002).

Hybrid machining

Hybrid machining means the combination of processes/techniques in order to produce parts in a more efficient and productive way (Lauwers, 2011). It should enhance the advantages and minimizes the potential disadvantages found in the individual techniques (Rajurkar et al., 1999). There is not much research in hybrid machining of titanium alloys. (Dandekar et al., 2010) investigated hybrid machining of Ti–6Al–4V by including heating of workpiece and cryogenic cooling of the tool simultaneously. The machining process took the advantages of softening the workpiece by heating and reducing tool degradation by cooling. Generally laser heating is used for softening the workpiece and a liquid nitrogen circulation is used for cooling the cutting tool. Two to three times longer tool life at higher cutting speeds (150–200 m/min) can be achieved by this method. A TiAlN coated carbide cutting tool performs 2–3 times better than an uncoated carbide tool for hybrid machining of Ti–6Al–4V at all cutting speeds (Dandekar et al., 2010). There are several reasons of improved machinability in hybrid machining of titanium alloy, such as (1) heated workpiece becomes softer and machining forces/pressure load reduce, (2) continuous chips are produced at higher speed which reduces the variation of chip thickness and thus machining forces and (3) cooling of cutting tool reduces the diffusion wear and retains the strength of cutting tool.

Dandekar et al., (2010) did not find discernible difference in the machined micro-structure and the microhardness between conventional machining and hybrid machining. An economic analysis was also carried out based on estimated tooling and labour costs. It was found that the hybrid process with a TiAlN coated tool shows a considerable improvement in machinability of Ti–6Al–4V through increased material removal rate and increased tool life. It could yield a 40% reduction in overall machining costs (Dandekar et al., 2010).

Finish cut and wait-machine

For spring back problems the workpiece at the cutting tool tip moves away and reduce the depth of cut. The material come backs to original position when the cutting tool passed. This can be minimised by using a sharp cutting tool and adding few extra finish cut operations. The sharp cutting tools remove material by applying very little force which reduces the

deflection of workpiece. On the other hand, each finish cut will remove part of the total depth of cut at a time. Thus, repetitive finish cut removes the total depth of cut at a certain stage. For example, if there are 2 operations to machine the part complete then it is necessary to add an extra 2 operations for roughing only. To release the stress, in the first finishing operation after roughing it requires shim any gaps in between the part and the fixture where it is clamped to eliminate any spring back in the part. In addition, the workpiece can be rested for several days if time allows, but shimming would still be required.

(Islam et al., 2013) investigated several cutting parameter, such as coolant type, cutting speed and feed rate on dimensional accuracy of cylindrical titanium bar. This study shows that proper selection of the cutting parameters may counter affect the spring back problems. It concluded that the cooling method moderately influences diameter error (contribution ratio 25.00 %) and cryogenic cooling provides least diameter error when combined with higher cutting speed and medium-feed rate. Cooling method significantly affects circularity (contribution ratio 76.75 %). Dry machining and a combination of feed rate and cutting speed provide optimum circularity due to local softening and chip formation mechanism. Generally elasticity reduces with the reduction of temperature and materials tend to be brittle at low temperature. Thus spring back effect for dimensional error reduces by the cryogenic cooling. On the other hand, the circularity is much more sensitive than dimensional error. It seems the effect of significant temperature difference due to cryogenic cooling disturbs the circularity.

(Islam et al., 2013a) recognized (a) an overcut of material opposite the position of each jaw of the three-jaw chuck, and (b) an undercut of material along the position of each jaw as the primary causes of circularity error. The change of radial cutting force direction with respect to the jaw positions also contributes to circularity error (Islam et al., 2013a). The radial stiffness and the stability of the workpiece are affected by cutting speed and feed rate (Islam et al., 2013). Higher feed rate produces higher forces that contributes the under/over cut. The machining processes are generally less stable at higher cutting speed which cause the under/over cut. At lower cutting speeds, the mechanism of titanium failure within the upper region of the primary shear zone appears to be cleavage (Barry et al., 2001). This behavior apparently results in ductile fracture. Shear localization during titanium machining results in a cyclic variation of forces (both cutting and thrust) with a significant variation in magnitude (Komanduri et al., 2002). Therefore, the circularity which is generally affected by radial force and elasticity of the workpiece material is indirectly related to localized softening

(due to localized heat generation) and chip formation mechanism (Pramanik et al., 2013). The optimum local softening and chip formation mechanism for best circularity are achieved by the combined effects of feed and cutting speed. Thus the introduction of flood and cryogenic cooling destabilizes the heating and cooling processes (Islam et al., 2013).

If the residual stress is too high in the workpiece then it should be machined step by step by removing materials from tensile side first. In addition, all titanium alloys can be stress relieved without affecting their mechanical properties. Combinations of time and temperature can be used to remove the stress. Thicker sections require longer times to insure uniform temperatures. Either furnace or air cooling is usually acceptable. The cooling rate is not critical but uniformity of cooling is important (Campbell, 2006).

Other methods

Spindle speed variation (SSV) is a chatter suppression technique that can break the regenerative effect to avoid the growth of vibrations through a continuous and controlled modulation of spindle speed (Weck et al. 1975). It is noted that SSV technique is more effective when comparatively lower cutting speeds applied (Quintana and Ciurana 2011). Although introduction of SSV mitigates vibrations, its application in the industries is still limited (Siddhpura et al., 2012) as it requires an additional spindle torque and higher energy consumption. The lack of a deep knowledge on the mechanics involved in the material removal process when the SSV is adopted still represents a major obstacle to a broad diffusion of the technique. In order to bridge part of the knowledge gap Albertelli et al. (2012) studied the effect of spindle modulation on tool life during turning steel. It was noted that the variation spindle speed reduces the tool life when applied in stable conditions. Albertelli et al. (2012) applied sinusoidal spindle speed variation (SSSV) in turning process. They noted that the SSSV did not influence the surface finish negatively even when it was applied during a stable turning operations. Bediaga et al., (2011) tested effectiveness of the continuous spindle speed variation (CSSV) technique as a chatter-suppression strategy in the milling process. They proposed a stability map for different amplitude and frequency variations in order to optimize the parameter selection when machining. Chiappini et al., (2014) found that the engagement between tool and workpiece changes with the modulation chip thickness. The production of heat and the heat flow in the tool and workpiece depends on the tool-workpiece engagement. For the bigger chip thickness, heat is diffused through

bigger tool-workpiece contact length but the length of the contact becomes limited when the chip thickness becomes smaller. This is also true for tool-material contact pressure. The contact pressure exhibits a relevant oscillation during SSSV period. The highest thermal load and the highest contact pressure do not occur at the same time and in the same tool-material contact region (Chiappini et al., 2014). Thus a thermo-mechanical cycle appears that might fatigue the tool in variable speed and, highest peaks of pressure and temperatures are reached. Thus a variable cutting speed reduces tool life in stable conditions.

The application of variable pitch cutting tools is another way to reduce chatter during milling of titanium alloy. These tools possess non-uniform helix and pitch (as shown in Fig. 1) to disrupt chatter vibration. Variable helix tools can be designed to provide substantial performance improvements compared to traditional tools, due to their improved chatter stability (Yusoff et al., 2011). Variable pitch tools were initially proposed by (Slavicek, 1965 and Opitz et al., 1966) had a higher stable depth of cut during machining with tools with irregular tooth pitches. (Altintas et al., 1999) utilized an invariant time constant and a non-uniform multiple regeneration time delay to optimise pitch geometry of variable pitch tools. (Olgac and Sipahi, 2007 and Budak, 2003) also modelled and optimised variable pitch tools. The optimisation process is complex due to the nonlinear relationship between the input and output variables. Material removal rate can be maximised by applying an optimised irregular pitch tool. (Yusoff et al., 2011) experimentally achieved a five-fold improvement in chatter stability by an optimized variable tool. The variable helix tools suffer from period-one chatter instability. Furthermore, the instability can occur in small isolated regions of the stability diagram, so that small changes in the process parameters can have a large effect on the stability (Yusoff et al., 2011).

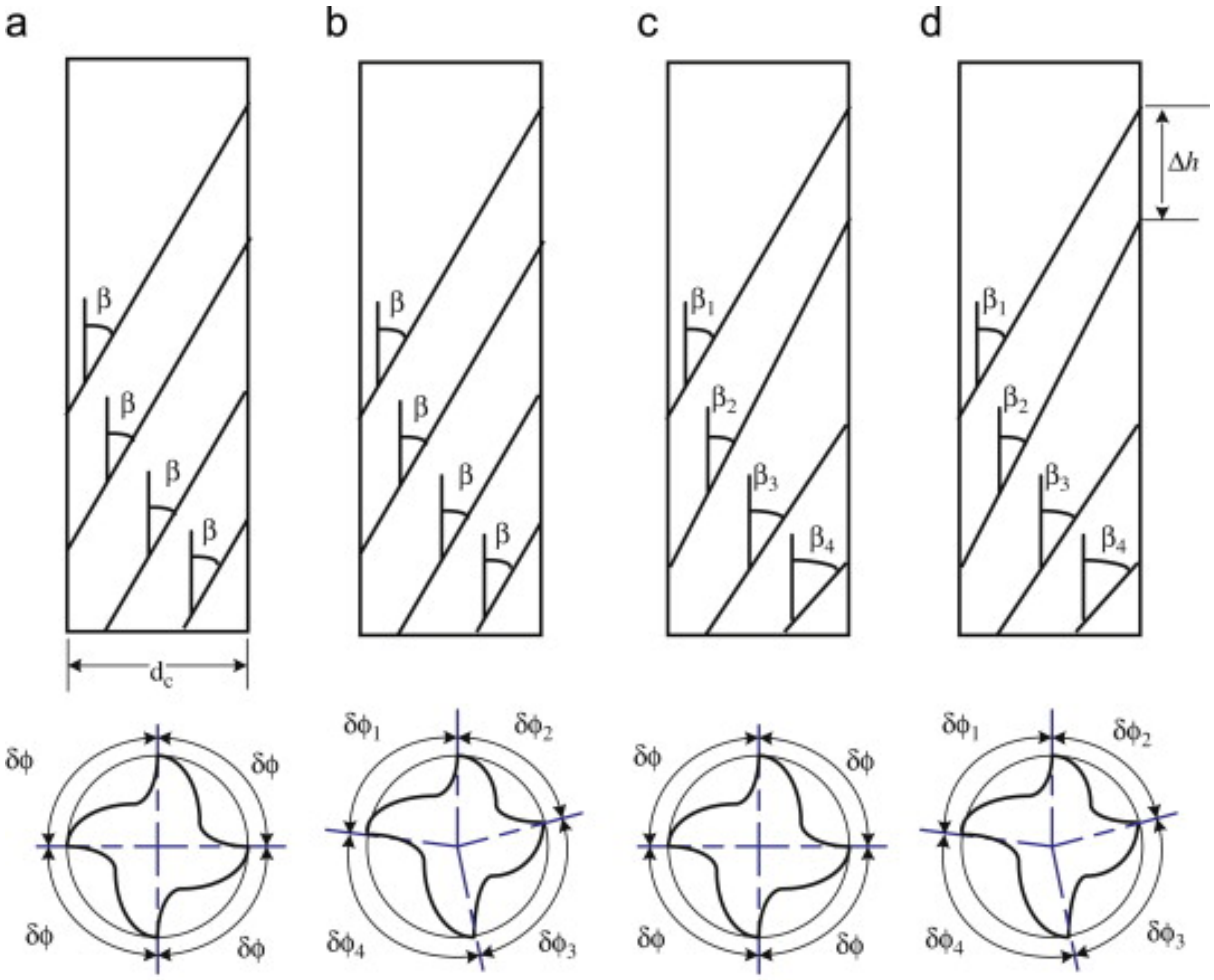

Fig. 16 Variable pitch tool geometry for a four flute tool: (a) regular tool−uniform pitch and uniform helix; (b) variable pitch tool; (c) variable helix tool−special case with regular pitch at the tool tip; and (d) variable helix tool (Yusoff et al., 2011).

CONCLUSION

Huge investigation has been performed to understand the machining and tool wear mechanisms to improve productivity of titanium machining processes. The two inherent properties, such as saw tooth chip formation and low thermal conductivity of titanium alloy are in the root of all complexity associate to machining of this material. The two properties are also related to each other. For example, low thermal conductivity induces local high temperature which contributes shear instability during chip formation. On the other hand saw tooth chip causes variation of chip thickness which causes variation of local temperature. Unfortunately, these two properties can't be changed. The remedies of the challenges of

machining titanium alloy come from adjusting cutting parameters and environments. The vibration analysis kit adjusts the natural vibration of machine tools with the self-excited vibration due the machining and minimizes the variation of chip thickness. At the current stage there is high potential of this method which is capable to improve productivity more than 100% during machining titanium. This method can increase axial depth of cut and speed by eliminating self-excited vibration. Thermally enhanced machining increase the critical cutting speed to start saw tooth chips. Thermal assisted machining looks promising but it is difficult to implement and make acceptable for industry application. Coolant and conductive cutting tool holder removes the heat from the cutting zones. So far the high pressure coolant is most efficient method to control the cutting temperature. Hybrid machining increases the critical cutting speed as well as retains strength of cutting tools. Finish cut and wait-machine improves the dimensional accuracy, and commonly used in the industries for machining titanium alloy.

REFERENCES

Abdel-Aal, H. A.; Nouari, M.; El Mansori, M. (2009) Influence of thermal conductivity on wear when machining titanium alloys, *Tribology International*, *42*(2): 359-372.

Ahmadi, K.; Ismail, F. (2012) Stability lobes in milling including process damping and utilizing Multi-Frequency and Semi-Discretization Methods. *International Journal of Machine Tools and Manufacture*, 54: 46-54.

Abele, E.; Fröhlich, B. (2008) High speed milling of titanium alloys. *Advances in production engineering and management*, 3: 131-140

Albertelli, P.; Mussi, V. ; Ravasio, C. ; Monno, M. (2012) An experimental investigation of the effects of spindle speed variation on tool wear in turning. *Procedia CIRP*, 4: 29–34.

Albertelli, P.; Musletti, S.; Leonesio, M.; Bianchi, G.; Monno, M. (2012) Spindle speed variation in turning: technological effectiveness and applicability to real industrial cases. *The International Journal of Advanced Manufacturing Technology*, 62: 59–67.

Altıntaş, Y.; Budak, E.; Engin, S. (1999) Analytical stability prediction and design of variable pitch cutters. *Journal of Manufacturing Science and Engineering*, 121(2): 173-178.

Bäker, M.; Rösler, J.; Siemers, C. (2002) A finite element model of high speed metal cutting with adiabatic shearing. *Computers & Structures*, *80*(5): 495-513.

Bayoumi, A.E.; Xie, J.Q. (1995) Some metallurgical aspects of chip formation in cutting Ti-6wt.%Al-4wt.%V alloy. *Materials Science and Engineering A*, 190: 173-180.

Barry, J.; Byrne, G.; Lennon, D. (2001) Observations on chip formation and acoustic emission in machining Ti–6Al–4V alloy. *International Journal of Machine Tools and Manufacture*, 41:1055–1070.

Bediaga, I.; Zatarain, M.; Muno,a J.; Lizarralde, R. (2011) Application of continuous spindle speed variation for chatter avoidance in roughing milling. *Proceedings of the Institution of Mechanical Engineers Part B: Journal of Engineering Manufacture*, 225:631–640.

Bermingham, M.J.; Palanisamy, S.; Kent, D.; Dargusch, M.S. (2012) A comparison of cryogenic and high pressure emulsion cooling technologies on tool life and chip morphology in Ti–6Al–4V cutting. *Journal of Materials Processing Technology*, 212: 752– 765.

Bouzakis, K.-D.; Michailidis, N.; Skordaris, G.; Kombogiannis, S.; Hadjiyiannis, S. .; et al. (2002) Effect of the Cutting Edge Radius and its Manufacturing Procedure on the Milling Performance of PVD Coated Cemented Carbide Inserts. *Annals of the CIRP*, 51(1):61‑64.

Barry, J.; Byrne, G. (2001) Study on acoustic emission in machining hardened steels. Part 1: acoustic emission during saw-tooth chip formation. *Proceedings of the Institution of Mechanical Engineers Part B: Journal of Engineering Manufacture*, 215: 1549–1559.

Bareggi, A.; O'donnell, G.E.; Torrance, A. (2008) Modelling and experimental analysis of high speed air jets used during metal cutting as a cooling technique. *Proceedings of the Third CIRP International Conference on High Performance Cutting*, 1: 337–346.

Budak, E. (2003). An analytical design method for milling cutters with nonconstant pitch to increase stability, part I: theory and part 2: application. *Journal of Manufacturing Science and Engineering*, *125*(1), 29-38.

Campbell, F.C. (2006) Manufacturing Technology for Aerospace Structural Materials, 1st edition, Elsevier Ltd.

Chiappini, E.; Tirelli, S.; Albertelli, P.; Strano, M.; Monno, M. (2014) On the mechanics of chip formation in Ti-6Al-4V turning with spindle speed variation. *International Journal of Machine Tools and Manufacture*, 77:16–26.

Coz, G.L.; Marinescu, M.; Devillez, A.; Dudzinski, D.; Velnom, L. (2012) Measuring temperature of rotating cutting tools: Application to MQL drilling and dry milling of aerospace alloys. *Applied Thermal Engineering*, 36: 434-441.

Chichili, D.R.; Ramesh, K.T.; Hemker, K.J. (1998) The high-strain-rate response of alpha-titanium: Experiments, deformation mechanisms and modelling. *Acta Materialia*, 46: 1025–43.

Chiou, R. Y.; Liang, S.Y. (1998). Chatter stability of a slender cutting tool in turning with tool wear effect. *International Journal of Machine Tools and Manufacture*, *38*(4): 315-327.

Dearnly, P.A.; Grearson, A.N. (1986) Evaluation of principal wear mechanisms of cemented carbides and ceramics used for machining titanium alloy IMI 318. *Material Science and Technology*, 2: 47–58.

Dandekar, C.R.; Shin, Y.C.; Barnes, J. (2010) Machinability improvement of titanium alloy (Ti-6Al-4V) via LAM and hybrid machining. *International Journal of Machine Tools and Manufacture*, 50(6): 174–182.

Dhananchezian, M.; Pradeep, K.M. (2011). Cryogenic turning of the Ti–6Al–4V alloy with modified cutting tool inserts. *Cryogenics*, 51(1): 34-40.

Ding, H.; Shen, N.; Shin, Y.C. (2012) Thermal and mechanical modeling analysis of laser-assisted micro-milling of difficult-to-machine alloys. *Journal of Materials Processing Technology*, 212: 601– 613.

Donachie Jr., M.J. (1988) Titanium: A Technical Guide, ASM International, Material Park, OH.

Duan, C.; Zhang, L. (2013) A reliable method for predicting serrated chip formation in high-speed cutting: analysis and experimental verification. *The International Journal of Advanced Manufacturing Technology*, 64(9-12): 1587-1597.

Ezugwu, E.O. (2004) High speed machining of aero-engine alloys, *Journal of the Brazilian Society of Mechanical Sciences & Engineering*, 26:1–11.

Ezugwu, E.O.; Silva, R.B.D.; Bonney, J.; Machado, Á.R. (2005) Evaluation of the performance of CBN tools when turning Ti–6Al–4V alloy with high pressure coolant supplies. *International Journal of Machine Tools & Manufacture*, 45: 1009–1014.

Ezugwu, E.O. (2007) Improvements in the machining of aero-engine alloys using self-propelled rotary tooling technique. *Journal of Materials Processing Technology*, 185: 60–71.

Ezugwu, E.O.; Wang, Z.M. (1997) Titanium alloys and their machinability — a review. *Journal of Materials Processing Technology*, 68: 262-274.

Ezugwu, E.O.; Bonney, J.; Yamane, Y. (2003) An overview of the machinability of aeroengine alloys. *Journal of Materials Processing Technology*, 134: 233–253.

Ezugwu, E.O.; Bonney, J.; Silva, R.B.D.; Akir, C.O. (2007a) Surface integrity of finished turned Ti–6Al–4V alloy with PCD tools using conventional and high pressure coolant supplies. *International Journal of Machine Tools & Manufacture*, 47: 884–891.

Fan, Y.; Zheng, M.; Zhang, D.; Yang, S.; Cheng, M. (2011) Static and dynamic characteristic of cutting forces when high efficiency cutting Ti-6Al-4V. *Advanced materials research*, 305: 122-128.

Friedrich, C.R.; Kulkarni, V.P. (2004) Effect of workpiece spring back on micromilling forces. *Microsystem Technologies*, 10: 472–477

Follansbee P.; Gray, G.T. (1989) An analysis of the low temperature, low and high strain-rate deformation of Ti-6Al-4V. *Metallurgical Transactions A*, 20: 863–874.

Ginting, A.; Nouari, M. (2006) Experimental and numerical studies on the performance of alloyed carbide tool in dry milling of aerospace material. *International Journal of Machine Tools & Manufacture*, 46: 758–768.

Gente, A.; Hoffmeister, H.W.; Evans, C. J. (2001) Chip formation in machining Ti6Al4V at extremely high cutting speeds. *CIRP Annals-Manufacturing Technology*, *50*(1): 49-52.

Haron, C.H.C.; Ginting, A.; Arshad, H. (2007) Performance of alloyed uncoated and CVD-coated carbide tools in dry milling of titanium alloy Ti-6242S. *Journal of Materials Processing Technology*, 185: 77–82.

Haron, C.H.C. (2001) Tool life and surface integrity in turning titanium alloy. *Journal of material processing technology*, 118: 231-237.

Hartung, P.D.; Kramer, B.M.; Von Turkovich, B.F. (1982) Tool wear in titanium machining. *CIRP Annals-Manufacturing Technology*, *31*(1): 75-80.

Hong, S.Y.; Ding, Y. (2001). Cooling approaches and cutting temperatures in cryogenic machining of Ti-6Al-4V. *International Journal of Machine Tools and Manufacture*, 41(10): 1417-1437.

Hou, Z.B.; Komanduri, R. (1997) Modeling of thermomechanical shear instability in machining. *International Journal of Mechanical Sciences*, *39*(11): 1273-1314.

Hirosaki, K.; Shintani, K.; Kato, H.; Asakura, F.; Matsuo, K. (2004) High Speed Machining of Bio-Titanium Alloy with a Binder-Less PCBN Tool. *JSME International Journal Series C*, 47(1): 14-20

Huang, C.Y.; Wang, J.J. (2007) Mechanistic modeling of process damping in peripheral milling. *Journal of Manufacturing Science and Engineering*, *129*(1): 12-20.

Islam, M.N.; Anggono, J.M.; Pramanik, A.; Boswell, B. (2013). Effect of cooling methods on dimensional accuracy and surface finish of a turned titanium part. *The International Journal of Advanced Manufacturing Technology*, 69(9-12): 2711-2722

Islam, M. N. (2013a). Effect of Additional Factors on Dimensional Accuracy and Surface Finish of Turned Parts. *Machining Science and Technology*, *17*(1): 145-162.

Jawaid, A.; Che-haron, C.H.; Abdullah, A. (1999) Tool wear characteristics in turning of titanium alloy Ti-6246. *Journal of material processing technology*, 92–93: 329–334.

Komanduri, R.; Hou, Z.-B. (2002) On the thermoplastic shear instability in the machining of atitanium alloy (Ti–6Al–4V). *Metallurgical and Materials Transactions*, 33A: 2995–3010.

Kitagawa, T.; Kubo, A.; Maekawa, K. (1997) Temperature and wear of cutting tools in high-speed machining of Incone1718 and Ti-6A1-6V-2Sn. *Wear*, 202: 142-148

Kahles, J.F.; Field, M.; Eylon, D.; Froes, F.H. (1985) Machining of titanium alloys. *Journal of Metals*, 37(4): 27-35.

Kuljanic, E.; Fioretti, M.; Beltrame, L.; Miani, F. (1998) Milling Titanium Compressor Blades with PCD Cutter. *CIRP Annals - Manufacturing Technology*, 47(1): 61–64

Komanduri, R.; Turkovich, B.F.V. (1981) New observations on the mechanism of chip formation when machining titanium alloys. *Wear*, 6: 179–188.

Kikuchi, M. (2009) The use of cutting temperature to evaluate the machinability of titanium alloys. *Acta Biomaterialia*, 5: 770–775.

Komanduri, R. (1982) Some clarifications on the mechanics of chip formation when machining titanium alloys. *Wear*, 76: 15 – 34.

Kops, L.; Arenson, M. (1999) Determination of convective cooling conditions in turning. *Annals of the CIRP*, 48: 47–52.

Kovacevic, R.; Cherukuthota, C.; Mazurkiewicz. M. (1995) High pressure water jet cooling/lubrication to improve machining efficiency in milling. *International Journal of Machine Tools & Manufacture*, 35(10): 1459-1473.

Lin, Z.C.; Lo, S.P. (1997) A study of the tool-chip interface contact problem under low cutting velocity with an elastic cutting tool. *Journal of materials processing technology*, *70*(1): 34-46.

Lutjering, G.; Williams, J.C. (2003) Titanium, Springer, Berlin.

Lennon, A.M.; Ramesh, K.T. (2004) The influence of crystal structure on the dynamic behavior of materials at high temperatures. *International Journal of Plasticity*, 20: 269–290.

Lauwers, B. (2011) Surface integrity in hybrid machining processes. *Procedia Engineering*, 19: 241 – 251.

Lacalle, L.N.L.D.; Perez-Bilbatua, J.; Sanchez, J.A.; Lorente, J.I.; Alboniga, J. (2000) Using high pressure coolant in the drilling and turning of low machinability alloys. *International Journal of Advanced Manufacturing Technology*, 16: 85–91

Machado, A.R.; Wallbank, J.; Pashby, I.R.; Ezugwu, E.O. (1998) Tool performance and chip control when machining Ti6A14V and inconel 901 using high pressure coolant supply. *Machining Science and Technology: An International Journal*, 2(1):1-12

Nabhani, F. (2001) Machining of aerospace titanium alloys. *Robotics and Computer Integrated Manufacturing*, 17:99-106

Nandy, A. K.; Gowrishankar, M.C.; Paul, S. (2009) Some studies on high-pressure cooling in turning of Ti–6Al–4V. *International Journal of Machine Tools and Manufacture*, 49(2):182–198.

Obikawa, T.; Usui, E. (1996) Computational machining of titanium alloy—finite element modelling and a few results. *Journal of Manufacturing Science and Engineering-Transactions of the ASME*, 118: 208–215.

Olgac, N.; Sipahi, R. (2007). Dynamics and stability of variable-pitch milling. *Journal of Vibration and Control*, 13(7): 1031-1043.

Opitz, H.; Dregger, E.U.; Roese, H. (1966) Improvement of the dynamic stability of the milling process by irregular tooth pitch. *Proceedings of the Adv. Machine Tool Design and Research Conference* , 7: 213).

Palanisamy, S.; McDonald, S.D.; Dargusch, M.S. (2009) Effects of coolant pressure on chip formation while turning Ti6Al4V alloy. *International Journal of Machine Tools & Manufacture*, 49:739–743.

Palanisamy, S.; Townsend, D.; Scherrer, M.; Andrews R.; Dargusch, M.S. (2009a) High pressure coolant application in milling titanium. *Materials Science Forum*, 618-619: 89-92.

Pramanik, A; Islam, M.N; Basak, A; Littlefair, G. (2013) Machining and Tool Wear Mechanisms during Machining Titanium Alloys. *Advanced Materials Research*, 651: 338-343.

Pramanik, A. (2014). Problems and solutions in machining of titanium alloys. *International Journal of Advanced Manufacturing Technology*, 70(5-8): 919-928.

Quintana, G.; Ciurana, J. (2011) Chatter in machining processes: a review. *International Journal of Machine Tools & Manufacture*, 51: 363–376.

Ramesh, K.T. (2002) Effects of high rates of loading on the deformation behaviour and failure mechanisms of hexagonal close-packed metals and alloys. *Metallurgical and materials transactions A*, 33: 927–35.

Rech, J.; Yen, Y.C.; Schaff, M.J.; Hamdi, H.; Altan, T.; Bouzakis, K. D. (2005) Influence of cutting edge radius on the wear resistance of PM-HSS milling inserts. *Wear*, 259(7‑12):1168‑1178.

Rahman, M.; Wang, Z.G.; Wong, Y.S. (2006) A Review on High-Speed Machining of Titanium Alloys. *JSME International Journal Series C*, 49(1): 11-20.

Rahim, E.A.; Sasahara, H. (2011) A study of the effect of palm oil as MQL lubricant on high speed drilling of titanium alloys. *Tribology International*, 44: 309–317.

Rajurkar, K.P.; Zhu, D.; McGeough, J.A.; Kozak, J.; De Silva A. (1999) New Developments in ECM. *CIRP Annals – Manufacturing Technology*, 48(2): 567-579.

Shaw, M.C.; Dirke, S.O.; Smith, P.A.; Cook, N.H.; Loewen, E.G.; Yang, C.T. (1954) *Machining titanium* (No. AD-67971). Massachusetts Inst. of Tech., Cambridge. Dept. of Michanical Engineering.

Siddhpura, M.; Paurobally, R. (2012) A review of chatter vibration research in turning. *International Journal of Machine Tools & Manufacture*, 61: 27–47.

Smith, W.F. (1981) *Structure and Properties of Engineering Alloys*. McGraw-Hill, New York.

Schmitz T.L.; Smith, K.S. (2008) *Machining Dynamics- Frequency Response to Improve Productivity*. Springer, Dordrecht, ISBN9780387096452.

Sheikh-Ahmad, J.; Bailey, J.A. (1997) Flow instability in the orthogonal machining of CP titanium. *Journal of Manufacturing Science and Engineering-Transactions of the ASME*, 119 (3): 307-313

Strano, M.; Chiappini, E.; Tirelli, S.; Albertelli, P.; Monno, M. (2013) Comparison of Ti6Al4V machining forces and tool life for cryogenic versus conventional cooling. *Proceedings of the Institution of Mechanical Engineers, Part B: Journal of Engineering Manufacture*, 227(9): 1403-1408.

Shaw, M.C. (1984) *Metal Cutting Principles*. Clarendon, Oxford.

Shivpuri, R.; Hua, J.; Mittal, P.; Srivastava, A.K. (2002) Microstructure-mechanics interactions in modeling chip segmentation during titanium machining. *CIRP Annals - Manufacturing Technology*, 51(1): 71–74

Settineri, L.; Faga, M.G. (2008) Nanostructured cutting tools coatings for machining titanium. *Machining Science and Technology*, 12:158–169

Su, Y.; He, N.; Li, L.; Li, X.L. (2006) An experimental investigation of effects of cooling/ lubrication conditions on toolwear in high-speed end milling of Ti–6Al–4V. *Wear*, 261 (7–8): 760–766.

Semiatin, S.L.; Lahoti, G.D.; Oh, S.I. (1983) The occurrence of shear bands in metalworking. In *Material Behavior Under High Stress and Ultrahigh Loading Rates* (pp. 119-159). Springer US.

Sharma, V.S.; Dogra, M.; Suri, N.M. (2009) Cooling techniques for improved productivity in turning. *International Journal of Machine Tools & Manufacture*, 49: 435–453.

Slavicek, J. (1965). The effect of irregular tooth pitch on stability of milling. *Proceedings of the 6th Machine Tool Design and Research Conference*, 6: 15-22.

Sun, S.; Brandt, M.; Dargusch, M.S. (2009) Characteristics of cutting forces and chip formation in machining of titanium alloys. *International Journal of Machine Tools and Manufacture*, 49: 561–568.

Sun, S.; Brandt, M.; Dargusch, M.S. (2010) Thermally enhanced machining of hard-to-machine materials—A review. *International Journal of Machine Tools & Manufacture*, 50: 663–680.

Sun, S.; Brandt, M.; Dargusch, M.S. (2010a) The effect of a laser beam on chip formation during machining of Ti6Al4V alloy. *Metallurgical and Materials Transactions A*, 41: 1573–1581.

Sun, S.; Brandt, M.; Dargusch, M.S. (2010b) Machining Ti–6Al–4V alloy with cryogenic compressed air cooling. *International Journal of Tool & Manufacture*, 50: 933–942.

Sun, S.; Brandt, M.; Barnes J.E.; Dargusch, M.S. (2011) Experimental investigation of cutting forces and tool wear during laser-assisted milling of Ti-6Al-4V alloy. *Proceedings of the Institution of Mechanical Engineers, Part B: Journal of Engineering Manufacture*, 225: 1512.

Sutter, G.; Faure, L.; Molinari, A.; Ranc, N.; Pina, V. (2003) An experimental technique for the measurement of temperature fields for the orthogonal cutting in high speed machining. *International Journal of Machine Tools & Manufacture*, 43: 671–678

Takeyama, H.; Murakoshi, A.; Motonishi, S.; Narutaki, N. (1983) Study on machining of titanium alloys. *Annals of the ClRP*, 32 (1): 65–69

Turkovich, B.F.V.; Hartung, P.D.; Kramer, B.M. (1982) Tool wear in titanium machining. *Annals of the ClRP*, 31(1): 75-80.

Ulutan, D.; Özel, T. (2013) Determination of tool friction in presence of flank wear and stress distribution based validation using finite element simulations in machining of titanium and nickel based alloys. *Journal of Materials Processing Technology*, 213: 2217– 2237.

Vyas, A.; Shaw, M.C. (1999) Mechanics of saw-tooth chip formation in metal cutting. *Journal of Manufacturing Science and Engineering—Transactions of the ASME*, 211: 163–172.

Vyas, A.; Shaw, M.C. (1999) Mechanics of saw-tooth chip formation in metal cutting. *Journal of Manufacturing Science and Engineering—Transactions of the ASME*, 211: 163–172.

Venugopal, K.A.; Paul, S.; Chattopadhyay, A.B. (2007) Tool wear in cryogenic turning of Ti-6Al-4V alloy. *Cryogenics*, 47: 12–18

Wang, Z.G.; Wong, Y.S.; Rahman, M. (2005a) High-speed milling of titanium alloys using binderless CBN tools. *International Journal of Machine Tools and Manufacture*, 45(1): 105-114.

Wang, Z.G.; Rahman, M.; Wong, Y.S. (2005b) Tool wear characteristics of binderless CBN tools used in high-speed milling of titanium alloys. *Wear*, 258 (5-6): 752-758.

Weck, M.; Verhaag, E.; Gather, M. (1975) Adaptive control for face-milling operations with strategies for avoiding chatter vibrations and for automatic cut distribution. *Annals of the ClRP*, 24: 405–409.

Wu, D.W. (1989) A new approach of formulating the transfer function for dynamic cutting processes. *Journal of Engineering for Industry*, *111*(1): 37-47.

Wyen, C.-F.; Wegener, K. (2010) Influence of cutting edge radius on cutting forces in machining titanium. *CIRP Annals - Manufacturing Technology*, 59: 93‑96

Yasir, A.M.S.; Hassan C.H.; Jaharah A.G.; Nagi H.E.; Yanuar B.; Gusri A. (2009) Machinalibilty of Ti-6Al-4V under dry and near dry condition using carbide tools, *The Open Industrial and Manufacturing Engineering Journal*, 2: 1-9

Yusoff, A.R.; and Sims, N.D. (2011) Optimisation of variable helix tool geometry for regenerative chatter mitigation. *International Journal of Machine Tools and Manufacture*, 51 (2): 133-141.

Zhen-Bin, H.; Komanduri, R. (1995) On a thermo-mechanical model of shear instability in machining. *Annals of the ClRP*, 44 (1): 69–73.

Zareena, A.R. (2002) *High-speed machining of titanium alloys*, Master Thesis, National University of Singapore, Singapore.

Zareena, A.R.; Veldhuis, S.C. (2012) Tool wear mechanisms and tool life enhancement in ultra-precision machining of titanium. *Journal of Materials Processing Technology*, 212: 560– 570

Zhang, Y. C.; Mabrouki, T.; Nelias, D.; Gong, Y.D. (2011) Chip formation in orthogonal cutting considering interface limiting shear stress and damage evolution based on fracture energy approach. *Finite Elements in Analysis and Design*, *47*(7): 850-863.

Zhang, Y.; Mabrouki, T.; Nelias, D.; Courbon, C.; Rech, J.; Gong, Y. (2012) Cutting simulation capabilities based on crystal plasticity theory and discrete cohesive elements. *Journal of Materials Processing Technology*, *212*(4): 936-953.